C.P. No. 922

C.P. No. 922

MINISTRY OF AVIATION

AERONAUTICAL RESEARCH COUNCIL

CURRENT PAPERS

Investigation of the Normal Force Characteristics of Slender Delta Wings with Various Rhombic Cross-Sections in Subsonic Conical Flow

by

D. L. I. Kirkpatrick

LONDON: HER MAJESTY'S STATIONERY OFFICE

1967

PRICE 10*s* 6*d* NET

U.D.C. No. 533.693.3 : 533.6.013.13 : 533.692.2 : 532.517.43 : 533.6.011.32/34

C.P. No.922*
December 1965

INVESTIGATION OF THE NORMAL FORCE CHARACTERISTICS OF SLENDER DELTA WINGS WITH VARIOUS RHOMBIC CROSS-SECTIONS IN SUBSONIC CONICAL FLOW

by

D. L. I. Kirkpatrick

SUMMARY

This report describes an experimental technique which was developed to determine the aerodynamic normal forces associated with the conical flow fields round slender wings at incidence. With this experimental technique it is possible to obtain the accurate information necessary for the investigation of the theoretical similarity of the conical flow fields round slender wings with different cross-sectional shapes. The report presents the results of the tests on four low-aspect-ratio wings with rhombic cross-sections whose leading-edge angles were $\pi/6$, $\pi/3$, $\pi/2$ and $2\pi/3$. These results show that the development with incidence of the normal force is appreciably affected by the magnitude of the leading-edge angle. The normal force component associated with the leading-edge vortices, which are characteristic of the flow round slender wings, develops much more slowly with incidence when the edge angle is large than when it is small. As the leading-edge angle is reduced, the slope of the normal force characteristic at zero incidence increases in the manner predicted by slender body theory, though the measured values are slightly smaller than those predicted.

---

*Replaces R.A.E. Tech. Report No.65291 - A.R.C.27990

CONTENTS

		Page
1	INTRODUCTION	3
2	EXPERIMENTAL EQUIPMENT AND PROCEDURE	5
	2.1 Description of models	5
	2.2 Support rig	6
	2.3 Force-measuring equipment	7
	2.4 Experimental procedure	8
3	RESULTS AND DISCUSSION	8
	3.1 Calculation of results	8
	3.2 Effects of the spanwise gap	9
	3.3 Discussion of results	11
4	CONCLUSIONS	14
Appendix A	Blockage corrections	16
Appendix B	Constraint corrections	19
Appendix C	Sting bar and balance deflection corrections	20
Tables		21-30
Symbols		31
References		32
Illustrations		Figures 1-15
Detachable abstract cards		-

1 INTRODUCTION

Since early tests on slender wings revealed that their lift at moderate to high incidences was considerably greater than had been predicted by simple cross-flow theories, it has been found that the flow field round a slender wing at such incidences is dominated by a vortex system which is associated with boundary-layer separation at the leading edges. Because this vortex system has an important effect on the aerodynamic characteristics of the slender wing it has been the subject of many theoretical studies and experimental investigations, but its structure, properties and development are still not fully understood. There is still no reliable method predicting the development of the vortex system above a slender wing as its incidence is increased, and hence of calculating accurately the aerodynamic forces and moments on it. But recently Maskell has produced a similarity theory* which will enable the development of the flow field round a whole class of slender wings to be predicted, provided that the development of the field round one member of the class has been determined.

This theory considers the flow past a slender, conical wing with sharp leading edges as the sum of two velocity fields, the linear and the non-linear. The linear field is associated with the attached flow round the wing assumed to occur in slender wing theory[2], and yields an aerodynamic normal force which is directly proportional to the angle of incidence. The theory suggests that the rate of change of this normal force with incidence is directly proportional to the wing's aspect ratio, and can be calculated for wings of any cross-sectional shape. The non-linear field is associated with the effects of flow separation at the leading edges, and is induced by the infinitely thin vortex sheets which spring from the leading edges of the wing and the sheets' reflections in the wing's surface. It is assumed that the interference between the two vortex fields near the leading edges is negligible, so the theory's applicability is restricted to the regime in which the distance of the vortex sheet from the leading edge is small compared to the lateral dimensions of the wing. Maskell's theory suggests that, close to the leading edge of a wing whose cross-section is symmetrical, the non-linear velocity field is dependent in form on the edge angle of the cross-section and on a generalized incidence parameter, and in magnitude on a scaling factor. This scaling factor and the incidence parameter are both functions of the geometrical incidence, the aspect ratio and the cross-sectional shape of the wing, and both can be calculated once the conformal transformation

---

*The ideas from which this theory was developed were first presented[1] at the Xth International Congress of Applied Mechanics at Stresa in 1960.

of the wing's cross-section into a circle is known; they can most easily be determined for wings whose cross-sections are bounded by straight lines or circular arcs. Hence, if the development with incidence of the linear and non-linear fields round a slender wing is known, the corresponding development of these fields round any other slender wing with the same edge angle can be derived, provided that the theoretical parameters are known for both wings

A programme of experiments is in progress at the R.A.E., Farnborough to test the validity of Maskell's similarity theory, as well as to investigate the development and effect of the leading-edge vortices above a slender delta wing at incidence in conical flow. This programme incorporates direct measurement of the normal force on a number of slender conical wings with different cross-sectional shapes, leading-edge angles and dihedral angles, and measurement of the positions of the leading-edge vortices which form above these wings at incidence. This report describes the means and methods used to determine the normal forces associated with the conical flow fields round such wings in subsonic flow, and presents the results of tests on the first series of wings to be tested. This series of wings, shown in Fig.1, was tested to discover the effect of the leading-edge angle of a wing's rhombic cross-section on its normal force characteristics and hence, by implication, the effect on the linear and non-linear flow fields round it.

Prior to the tests described in this report, an attempt[3] was made to investigate the development with incidence of the normal force on a slender wing in a conical flow field by measuring the static pressure distribution on the surface of a delta wing of aspect ratio 1·0 near its apex, where the flow field is virtually conical. This attempt was not successful because it proved impossible to measure the static pressure at enough points to define the distribution with sufficient accuracy, but the pressure distributions at different chordwise stations indicated that there was no appreciable non-conicality in the flow field round the front 40% of the wing. For the experiment described in this report, it was decided to use the inherently more accurate method of measuring directly the normal force on the front part of a slender delta wing. Each delta wing was therefore made in two parts, hereafter referred to as the fore-wing and the rear-wing, so that when the two parts were mounted in the tunnel the delta wing looked as if it had been sawn through to produce a narrow spanwise gap. The rear-wing was firmly bolted to a sting but the fore-wing was connected to the sting only by a simple two-component strain-gauge balance designed to measure the aerodynamic normal force and pitching moment on the fore-wing. The length of the fore-wing was chosen so that the conicality of

the flow field round it was influenced only by the small and calculable effects of the narrow spanwise gap. The normal forces and pitching moments measured by the strain-gauge balance were therefore associated with an almost conical flow field and the normal force characteristic associated with a conical flow field could be determined.

2 EXPERIMENTAL EQUIPMENT AND PROCEDURE

2.1 Description of models

Three conical wings were made for the tests described in this report. All three wings had rhombic cross-sections symmetrical about two perpendicular axes and the included angles at their leading edges were $\pi/6$, $\pi/3$ and $\pi/2$. The size and shape of the wings was determined primarily by the need to avoid excessive blockage or constraint effects of the wind-tunnel's walls on the flow round the wing. It was decided that the span of all the wings should be 14·4 inches, corresponding to a maximum base area of 104 sq in. and a maximum blockage correction to the wind-tunnel dynamic pressure of less than 5%, and that the aspect ratio of all the wings should be 0·8. If the aspect ratio were higher the region of conical flow at the front of the wing would be smaller; on the other hand if the aspect ratio were smaller than either the scale of the flow field would be inconveniently small or the wind-tunnel wall constraint corrections would be unacceptably large. Earlier experimental work[3] had suggested that the flow field round the front half of a conical delta wing of aspect ratio 0·8 should be virtually conical, so it was decided that the centre-line chord of each fore-wing should be 18 inches since the centre-line chord of the whole wing was 36 inches. Each rear-wing was made with a centre-line chord of 17·6 inches so that when the two parts of the wing were mounted in the wind-tunnel the wing looked as if it had been sawn through just behind the mid-chord point to produce a spanwise gap 0·4 inches wide. For each wing several shims were made with various thicknesses up to 0·390 inches and were shaped so that they could be fitted on to the front surface of the rear-wing without destroying its conicality and the wing could be tested with the spanwise gap between its two parts at various widths from 0·400 to 0·010 inches (see Fig.2). Inside each fore-wing a metal plate, to which the strain-gauge balance was attached, was located 10·8 inches from the apex of the fore-wing and perpendicular to its centre line. Great care needed to be taken in the construction and alignment of this plate when the wing was being made, and in attaching the plate to the strain-gauge balance when the wing was being mounted in the wind-tunnel, to ensure that during the tests the wing was conical, i.e. that the surfaces of the fore-wing lay in the same planes as the corresponding surfaces of the rear-wing.

The wings were made, with tolerances of ±0·005 inch on the overall dimensions, mostly of araldite and glasscloth because this material is lighter than metal and does not shrink or warp as does wood.

The wing of leading-edge angle $\pi/3$ was made so that it could be mounted with its major axis either horizontal or vertical in the wind-tunnel and so it could be used to investigate the development of the aerodynamic normal force on both a wing of leading-edge angle $\pi/3$ and aspect ratio 0·8 and a wing of leading-edge angle $2\pi/3$ and aspect ratio 0·462. In the discussion of the results, a wing whose leading-edge angle and dihedral angle are (for example) $\pi/6$ and zero respectively is designated $\frac{\pi}{6}/0$, and the results of tests on the wing of leading-edge angle $\pi/3$ mounted in its two different attitudes are considered as the results of tests on two separate wings, $\frac{\pi}{3}/0$ and $\frac{2\pi}{3}/0$.

2.2 Support rig

The wings were mounted successively in the wind-tunnel on a new support rig (see Fig.3) which has been designed by Kettle[4]. This rig permits the angles of roll and incidence of the wing under test to be selected and set with a nominal accuracy of 0·01 deg. and to be changed while the wind-tunnel is in operation. The accuracy of the incidence-measuring unit was checked during some tests made at low incidence with the force-measuring equipment set at its highest sensitivity. During these tests, the normal force on each wing was measured at intervals of 1/4 deg. as the incidence was increased from zero to 3 deg., then decreased from +3 to -3 deg. and finally increased from -3 to zero deg. During each of these three phases, the direction of change of the incidence was kept constant, i.e. while the incidence was being changed from zero to +3 deg. the angle of incidence was never decreased. The results (a typical set is plotted in Fig.4) showed that the actual incidence of the wing was about 0·03 deg. greater or less than the incidence indicated by the dial, corresponding to the continuous decrease or increase of the incidence, because of a lag between the movement of the sting and the incidence transducer. The accuracy of the results obtained using this rig can therefore be greatly increased if during the tests the direction of change of incidence is altered only at the extremities of the incidence range and no attempt is made to set the incidence of the wing at a chosen value by successive small positive and negative changes of its incidence. This procedure was used for the tests on each of the wings at low incidence where the accuracy of the incidence measurement is especially important.

2.3 Force-measuring equipment

The strain-gauge balance was machined from a solid steel bar and four matched pairs of cropped AB 11 strain gauges of the Baldwin S.R.4 type, whose performance has been discussed by Anderson[5], were used to form the difference and additive bridges used to measure the normal force and pitching moment coefficients respectively. A calibration revealed that the relation between the balance readings and the applied forces was linear over the range of forces and moments to be measured, and that the interaction between the normal force and pitching moment was negligible.

The signals from the two strain-gauge bridges were measured and recorded by the measuring units, with full automatic balancing and freeze facilities, recently installed in the 4 ft × 3 ft wind-tunnel. These units measure and record the signals from the strain-gauge balance simultaneously and enable measurements of forces and moments to be made very quickly; they have already been described in detail by Cole and Mitchell[6]. The units each incorporate an amplifier to amplify the signal from the strain-gauge and a potentiometer, graduated in 1000 divisions, to measure the change in the magnitude of the signal. The measurement is digitised and recorded by a typewriter, a card punch and a tape punch. Because of the inherent limitations in any digitising process, the results of a test over a range of incidence at a constant sensitivity setting have a greater possible percentage error at low incidences than at high incidences, so it was necessary to make a special test at low incidences with the sensitivity of the measuring equipment set as high as possible in order to define the low-incidence end of the normal force characteristic.

The design of the strain-gauge balance was determined primarily by the necessity of preventing unacceptable deflections of the fore-wing relative to the rear-wing during the tests. This requirement made it necessary for the maximum stress level in the balance to be appreciably lower than is usual. Because at low incidences the stresses in the balance were very small, and because the range of the measuring equipment's sensitivity control is naturally limited, it was not possible to obtain the desired amplification of the signals from the strain gauges and the scatter of the results of tests made at low incidence could not entirely be eliminated (see Fig.10). However, by taking and repeating a sufficient number of measurements, a close approximation to the normal force characteristic at low incidence was obtained.

2.4 Experimental procedure

To find the effect of the spanwise gap on the flow round the fore-wing, different shims were fitted successively to the front surface of the rear-wing, and the aerodynamic normal forces on the fore-wing at several incidences between 10 and 15 deg. were measured with the gap between the two parts of the wing set at various different widths. From these results the value of the correction for the effect of the gap on the conicality of the flow round the fore-wing was estimated. Using these measured values of the normal force, the deflection at high incidences of the fore-wing relative to the rear-wing was estimated and hence the smallest width of the gap which would preclude any physical contact between them during the experiment was calculated. The gap was then set at a slightly greater width by fitting the appropriate shim to the rear-wing and the aerodynamic normal forces and pitching moments on the fore-wing at incidences spaced one degree apart between -5 and +15 deg. were measured. The normal forces were also measured at incidences spaced about 1/4 deg. apart between -3 and +3 deg. with the sensitivity of the force-measuring equipment set at its maximum value to try to define the low-incidence end of the normal force characteristic. This process was repeated for each of the wings tested.

The tests were made in the 4 ft by 3 ft low-turbulence wind-tunnel at Farnborough at a wind speed of 120 fps at which speed it was found, by flow visualization tests on each wing at several incidences through the range (see Fig.5 for example), that the flow over the surface of the wings remained laminar back to the rear of the fore-wing unless transition was artificially stimulated by roughness. All the force-measuring tests were made at this wind speed of 120 fps so that the flow over the surface of each of the wings would be laminar and the results of the tests on different wings could usefully be compared. The wings were not tested at higher wind speeds where transition of the boundary layer would occur, or with their surfaces roughened to induce transition, because the consequent non-conicality of the flow field would invalidate the results of such tests.

3 RESULTS AND DISCUSSION

3.1 Calculation of results

The values at different incidences of the normal force and pitching moment on each fore-wing were calculated using the readings from the automatic force-measuring equipment and non-dimensionalised with respect to qS and qSc respectively, where q is the dynamic pressure in the wind-tunnel, S is the area

bounded by the leading edges and the base of the fore-wing, and c is its centre-line chord. The coefficients were then corrected for the effects of wind-tunnel blockage and constraint; because of the unusual character of this experiment the corrections were specially calculated as described in Appendices A and B respectively. The angles of incidence read from the support rig dials were corrected for the constraint effect of the wind-tunnel's walls and for the deflection of the sting bar and strain-gauge balance under load; the calculation of these corrections is described in Appendices B and C.

The values of the pitching moment coefficient C_M for each wing, measured at various incidences with the narrowest possible spanwise gap between the wing's two parts, were then divided by the corresponding values of the normal force coefficient C_N in order to find x', the distance from the apex of the fore-wing to the line of action of the normal force on it. The calibration of the strain-gauge balance had shown that, when it was fitted to the fore-wing, its centre of moment was located 15·5 inches from the apex so

$$\frac{x'}{c} = \frac{15{\cdot}5}{18} - \frac{C_M}{C_N}$$

$$= 0{\cdot}861 - \frac{C_M}{C_N} \quad .$$

The value of x'/c for each wing is an indication of the conicality of the flow round the wing, as discussed in the following section.

The values of C_N, C_M and x'/c obtained from the tests on the four wings with the narrowest possible gaps between their two parts are tabulated in Tables 1 to 4.

3.2 Effects of the spanwise gap

When these tests were planned, it was hoped that the effect on the flow field round the fore-wing of the narrow spanwise gap between it and the rear-wing would be small, and that the flow field would be virtually conical. But it was appreciated that, if the gap caused significant non-conicality in the flow field, the results of the tests could not safely be used to test Maskell's similarity theory of leading-edge vortex development. Consequently for each wing the different characteristics obtained from tests with the gap between the two parts of the wing set at different widths were first studied to determine the effect of the gap. Fig.6 shows the effect of varying the width of the spanwise gap on the normal force characteristic at high incidence for each of

the wings tested. It is clear that as the gap width is decreased its effect is lessened and the value of C_N approaches C_{N_c}, the value corresponding to a perfectly conical flow field round the wing. From the results of these tests the values of $\frac{dC_N}{d\delta}$ when $\delta = \delta_1$, where δ is the gap width and δ_1 is the minimum gap width used in the tests, were calculated at each incidence and used to find the mean value of $\frac{dC_N}{d\delta}$ when $\delta = \delta_1$, hereinafter written as $\left(\frac{dC_N}{d\delta}\right)_1$, for each wing. The values of C_{N_c} for each wing were then estimated using the expression

$$C_{N_c} = (C_N)_1 \left(1 + \frac{\delta_1}{(C_N)_1}\left(\frac{dC_N}{d\delta}\right)_1\right)$$

where $(C_N)_1$ is the value of the normal force coefficient measured when $\delta = \delta_1$. Since both δ_1 and $\left(\frac{dC_N}{d\delta}\right)_1$ are small, this expression should not be greatly in error unless there is a large change in the value of $\frac{dC_N}{d\delta}$ as δ tends to zero. The values of C_{N_c} thus obtained are given in Tables 1 to 4.

The smallness of the values of $\frac{\delta_1}{(C_N)_1}\left(\frac{dC_N}{d\delta}\right)_1$ for the wings tested suggests that, during the test when the gap width was at its minimum value, the flow round each of the wings was almost conical. This suggestion is supported by the corresponding values of x'/c, shown in Fig.7, which are all close to 2/3, the value associated with conical flow. It was expected that the effect of the gap would resemble the trailing-edge effect on the chordwise loading on a conventional slender wing and would decrease the value of x'/c below 2/3; this happens in the case of wings $\frac{\pi}{6}/0$ and $\frac{\pi}{3}/0$, but in the case of wings $\frac{\pi}{2}/0$ and $\frac{2\pi}{3}/0$ the values of x'/c were found to be slightly greater than 2/3. These latter values are probably influenced by an asymmetric distribution of pressure across the rear surfaces of the fore-wings of wings $\frac{\pi}{2}/0$ and $\frac{2\pi}{3}/0$ for in the case of these two wings the vertical dimensions of these surfaces are comparatively large.

Since the values of $\frac{\delta_1}{(C_N)_1}\left(\frac{dC_N}{d\delta}\right)_1$ for all four wings tested are small and the values of x'/c are close to 2/3 and do not vary with incidence, it is reasonable to assume that over the whole incidence range the values of C_{N_c} obtained as described above are very close to those associated with perfectly conical flow fields.

3.3 Discussion of results

The normal force characteristics of the four wings tested were plotted in Fig.8; it must be remembered when studying this figure that the aspect ratio of wing $\frac{2\pi}{3}/0$ is smaller than the aspect ratio of the other wings. Fig.8 shows that, as the leading-edge angle of a slender wing of rhombic cross-section increases, the aerodynamic normal force on the wing decreases considerably at all angles of incidence, as is shown by the table below.

Wing	K	Angle of incidence, degrees	C_{N_c}
$\frac{\pi}{6}/0$	0·2	5	0·127
		10	0·320
		15	0·572
$\frac{\pi}{3}/0$	0·2	5	0·107
		10	0·261
		15	0·470
$\frac{\pi}{2}/0$	0·2	5	0·087
		10	0·203
		15	0·351
$\frac{2\pi}{3}/0$	0·115	5	0·045
		10	0·102
		15	0·178

To obtain the wings' normal force characteristics independent of their aspect ratios, the values of $\frac{C_{N_c}}{K^2}$, where K is the cotangent of the sweepback angle of the leading edge, were plotted against α/K in Fig.9 for each of the four wings tested. This figure implies that at any value of α/K the variation of $\frac{C_{N_c}}{K^2}$ with leading-edge angle is virtually linear, so the curve of $\frac{C_{N_c}}{K^2}$ against α/K for a wing of zero thickness was estimated by linear extrapolation and plotted in Fig.9. Figs.8 and 9 both show that, for wings with rhombic cross-sections, the leading-edge angle of the wing's cross-section has a very important effect on the aerodynamic normal force characteristic. If this effect is of comparable importance for wings with other cross-sections, then it must certainly be taken into account, along with the aspect ratio, planform, etc., when estimating the performance of a low-aspect-ratio aircraft of non-zero thickness at subsonic speeds.

According to slender body theory, the normal force characteristic associated with conical flow round a slender wing with sharp leading edges is given by the expression

$$\frac{C_{N_c}}{K^2} = 2\pi a \left(\frac{\alpha}{K}\right) + f\left(\frac{\alpha}{K}\right)$$

where a is a constant dependent on the wing's cross-section and $f\left(\frac{\alpha}{K}\right)$ is an as yet unknown function of α/K. The normal force characteristics, which were determined by this experiment as described above and are associated with conical flow fields round wings with different rhombic cross-sections, were analysed to determine the functions a and $f\left(\frac{\alpha}{K}\right)$ for each of the wings tested.

To find first the values of $\frac{dC_{N_c}}{d\alpha}$ at zero incidence and hence experimental values of a, the values of $\frac{C_{N_c}}{\alpha}$ obtained from the tests on each of the four wings at small angles of incidence with the force-measuring equipment set at its maximum sensitivity were plotted against incidence in Fig.10. Using this method of plotting, the experimental results tend to scatter as the angle of incidence tends to zero, because of the inherent experimental inaccuracies discussed in section 2.3, so that it is difficult to define the value of a_{ex} for each wing independently. Therefore on each part of Fig.10 two bounding curves were drawn so that they enclosed a region containing the true normal force characteristic (as yet undefined) of each wing at low incidence. The points at which the bounding curves intercepted the $\frac{C_{N_c}}{\alpha}$ axis yield bounding values which form the limits of a range including the true value of a_{ex}. The bounding values of the range thus defined experimentally for each wing were divided by a_{th}, the value of a predicted for that wing by slender body theory, and plotted in Fig.11. The ranges for the three wings of aspect ratio 0·8 suggest that the value of $\frac{a_{ex}}{a_{th}}$ for this aspect ratio does not vary significantly with edge angle, and that to facilitate analysis of the results this value may be assumed to equal 0·945. Since only one wing of aspect ratio 0·462 was tested, the value of $\frac{a_{ex}}{a_{th}}$ for this aspect ratio was assumed to be 0·972, the mid-point of the range between the bounding values. These values of $\frac{a_{ex}}{a_{th}}$ were subsequently used at the beginning of the analysis of the shape of the normal force characteristic. After the values of $\frac{a_{ex}}{a_{th}}$ had been selected, curves were drawn through the points plotted in Fig.10(a),(b),(c) and (d) so that for each

wing the chosen curve intercepted the $\frac{C_{N_c}}{\alpha}$ axis at a point corresponding to the chosen value of $\frac{a_{ex}}{a_{th}}$. It seems probable that the differences between these chosen curves and the true curves of the normal force characteristic are insignificant.

The values of $\frac{C_{N_c}}{\alpha}$ obtained from normal force measurements over the whole range of incidence from zero to 15 deg. were plotted in Fig.12 and curves were drawn through the plotted points so that at low incidence they corresponded with the chosen curves shown in Fig.10. It is clear that at all angles of incidence the non-linear component of the normal force is affected much more severely by the change in the leading-edge angle than is the linear component, as is shown by the table below.

Wing	K	α	C_{N_c} linear	C_{N_c} non-linear
$\frac{\pi}{6}/0$	0·2	5	0·094	0·033
		10	0·187	0·133
		15	0·281	0·291
$\frac{\pi}{3}/0$	0·2	5	0·086	0·021
		10	0·172	0·089
		15	0·257	0·213
$\frac{\pi}{2}/0$	0·2	5	0·078	0·009
		10	0·156	0·047
		15	0·234	0·117
$\frac{2\pi}{3}/0$	0·115	5	0·042	0·003
		10	0·084	0·018
		15	0·125	0·053

Fig.12 also shows that the shape of the $\frac{C_{N_c}}{\alpha}$ characteristic is different for the different wings tested, acquiring more upward curvature as the leading-edge angle is increased.

Since the aerodynamic normal force characteristics associated with conical flow round slender wings had not previously been accurately measured, it was decided to analyse the results of this experiment to discover whether they supported the hypothesis, postulated in earlier theoretical analyses[7,8], that such normal force characteristics are given by expressions of the form

$$\frac{C_{N_c}}{K^2} = 2\pi a \left(\frac{\alpha}{K}\right) + b \left(\frac{\alpha}{K}\right)^p$$

where a, b and p are functions of the cross-sectional shape of the wing. Analysis of the experimental results, using at the beginning the values of a_{ex} chosen from Fig.11, revealed that for each wing there was a value of p such that when $\frac{C_{N_c}}{\alpha}$ was plotted against α^{p-1} the curvature of a line drawn through the points was zero and, therefore, that the normal force characteristics are satisfied by the above expression. These values of p were found to be 1·9, 2·1, 2·3 and 2·8 for wings $\frac{\pi}{6}/0$, $\frac{\pi}{3}/0$, $\frac{\pi}{2}/0$ and $\frac{2\pi}{3}/0$ respectively. These values of p were then used to obtain a more accurate value of a_{ex} for each wing by plotting $\frac{C_{N_c}}{\alpha}$ against α^{p-1} and drawing a straight line through the points to intersect the $\frac{C_{N_c}}{\alpha}$ axis (see Fig.13). For the three wings of aspect ratio 0·8 these values of a_{ex} were not perceptibly different from the values chosen from Fig.11, but for wing $\frac{2\pi}{3}/0$ the value found by plotting $\frac{C_{N_c}}{\alpha}$ against $\alpha^{1·8}$ was slightly smaller than that previously chosen. Using the values of a_{ex} and p thus found, the value of b for each of the wings was calculated and the values of a_{ex}, b and p were tabulated in Table 6. The values of a_{ex}, b and p were plotted in Fig.14 which shows that as the leading-edge angle increases the linear component of the normal force decreases slowly and the non-linear component decreases very quickly. For example, as the size of the leading-edge angle increases from $\frac{\pi}{6}$ to $\frac{2\pi}{3}$ the linear component of the normal force drops by 23% but the non-linear component drops by more than 90% when $\alpha/K \leq 1$.

4 CONCLUSIONS

The results presented in this report show clearly that the experimental technique chosen yields accurate information on the development of the aerodynamic normal forces on slender wings in conical flow. The perfecting of such a technique for measuring the forces associated with a conical flow field is of considerable importance, since it is unlikely that an accurate and comprehensive theory predicting the forces on low-aspect-ratio wings can be developed without first establishing a theory for the conical flow round such wings.

The results also show that the normal force characteristic associated with conical flow round a slender wing of rhombic cross-section is given by an expression of the form

$$\frac{C_N}{K^2} = 2\pi a \left(\frac{\alpha}{K}\right) + b \left(\frac{\alpha}{K}\right)^p$$

where a, b and p are functions of the wing's cross-section. The variation of a, b and p with the size of the leading-edge angle has been determined from the experimental results which show that the size of the non-linear component of the normal force is much more severely affected by changes in the leading-edge angle than is the linear component. The values of a found experimentally are very close to those calculated using slender body theory, indicating that this theory forms a valid basis for Maskell's similarity theory. The experimental technique presented above will be used to determine the normal force characteristics of wings with the same leading-edge angle but different cross-sectional shapes, and hence to investigate the validity of the similarity theory itself.

Appendix A

BLOCKAGE CORRECTIONS

The blockage corrections which should be applied to the results of the wind-tunnel tests described in this report cannot be calculated using the conventional methods described by Pankhurst and Holder[9], because these methods are valid only for bodies which give rise to an essentially streamlined flow. Nor can the corrections be calculated using Maskell's blockage theory[10] for bluff bodies because the drag forces on the wings tested in this experiment were not measured. Furthermore, to correct the results of this experiment, it was necessary to know the chordwise variation of the blockage because the blockage correction used must be associated with the front half of the wing rather than with the whole wing. A simple method of finding the approximate chordwise distribution of the blockage effect on a conical body, solely from its size and shape, was therefore developed and is presented below.

It is assumed that a slender conical body, at negligible incidence to the free stream, induces perturbation velocities at its images in the wind-tunnel walls similar to those induced by a distribution of sources along the body's axis of symmetry and a sink infinitely far downstream. The strength of the sink and the strength and distribution of the sources are uniquely determined by the size and shape of the body. The total strength δm of the sources on an element $\delta x'$ of the axis of symmetry is assumed to be equal to the product of the free stream velocity and the increase in the cross-sectional area of the body between the chordwise stations denoted by x' and $x' + \delta x'$; hence

$$\delta m = 2 \frac{UB}{c^2} x' \, \delta x' \qquad (1A)$$

where U is the free stream velocity, c the length and B the base area of the body. The streamwise component of the perturbation velocity at a point (x,y) in the flow round the body due to this source element is therefore

$$dU_1 = \frac{UB}{2\pi c^2} \frac{(x-x') \, x' \, dx'}{(y^2 + (x-x')^2)^{3/2}} \qquad (2A)$$

and the component due to all the source elements along the body's axis of symmetry is

$$\Delta U_1 = \frac{UB}{2\pi c^2} \int_0^c \frac{(x-x')\,x'\,dx'}{[y^2 + (x-x')^2]^{3/2}}$$

$$= \frac{UB}{2\pi c^2} \left\{ \frac{c}{\sqrt{y^2 + (c-x)^2}} - \log \frac{\sqrt{y^2 + x^2} + x}{\sqrt{y^2 + (x-c)^2} + (x-c)} \right\}$$

$$= \frac{UB}{2\pi c^2} k_1 \left(\frac{x}{c}, \frac{y}{c} \right) . \qquad (3A)$$

The blockage correction ε_1 due to the source distribution is equal to the sum of the values of $\frac{\Delta U_1}{U}$ evaluated at all the images of the model in the wind-tunnel walls.

Therefore

$$\varepsilon_1 = \frac{B}{2\pi c^2} \sum_{\substack{m=-\infty \\ m=n\neq 0}}^{m=+\infty} \sum_{n=-\infty}^{+\infty} k_1 \left(\frac{x}{c}, \frac{b}{c} \sqrt{(m\lambda)^2 + n^2} \right) \qquad (4A)$$

where b is the breadth of the wind-tunnel and λ is the height/breadth ratio.

The strength of the sink downstream is equal to the sum of the strengths of all the source elements and can be found from the equation

$$m = \int_0^c 2 \frac{UB}{c^2} x'\,dx' = UB . \qquad (5A)$$

The streamwise velocity increment induced by this sink and its images in the wind-tunnel walls is

$$\Delta U_2 = \tfrac{1}{2} \frac{UB}{b^2 \lambda}$$

therefore

$$\varepsilon_2 = \frac{B}{2 b^2 \lambda} . \qquad (6A)$$

So the total blockage correction is

$$\varepsilon = \varepsilon_2 + \varepsilon_1 \left(\frac{x}{c} \right) . \qquad (7A)$$

The total blockage correction was calculated for the case of this set of wings whose centre-line chords are 36 inches mounted in the 4 ft by 3 ft wind-tunnel. Fig.15 shows ε/B as a function of x/c, and the blockage correction factors used to correct the experimental results are tabulated below.

BLOCKAGE CORRECTION FACTORS

Wing	ε/B	B	$(1+\varepsilon)^2$
$\frac{\pi}{6}/0$	0·029	0·193	1·012
$\frac{\pi}{3}/0$		0·417	1·024
$\frac{\pi}{2}/0$		0·720	1·043
$\frac{2\pi}{3}/0$		0·417	1·024

Appendix B

CONSTRAINT CORRECTIONS

When slender wings are tested in wind-tunnels such that the chord of the wing is not small compared to the height of the tunnel, the constraint corrections applied to the results of the tests must include a term to allow for the boundary induced curvature of the flow. Sune B. Berndt[11], using classical slender wing theory, has derived an expression for an additional upwash correction factor δ' which varies along the chord of the wing. For delta wings the expression for δ' is

$$\delta'(x) = \int_0^c f\left(\frac{x-\xi}{\sqrt{C}}\right)\left(\frac{\xi}{c}\right)^2 \frac{d\xi}{\sqrt{C}} - F\left(\frac{c-x}{\sqrt{C}}\right) \qquad (1B)$$

where C is the wind-tunnels cross-sectional area, c is the wing chord and f and F are two functions calculated by Berndt for a variety of closed rectangular test sections.

When calculating the corrections to be applied to the test data obtained as described above, it must be remembered that while the flow in the wind-tunnel is influenced by both the fore-wing and the rear-wing, it is the effect of constraint on the flow round the fore-wing that is required to correct the test data. The incidence correction is therefore given by

$$\Delta\alpha = [\delta_o + \delta'(c)] \frac{\bar{S}}{C} \bar{C}_L \qquad (2B)$$

where δ_o is the lifting line upwash correction, c is the centre-line chord of the fore-wing, and $\bar{S}$ and $\bar{C}_L$ are respectively the area and lift coefficient of the whole wing. It was found, by substituting the appropriate values, that

$$\Delta\alpha = 0{\cdot}0129\ \bar{C}_L \ . \qquad (3B)$$

Similarly the pitching moment correction is given by

$$\Delta C_M = \left(\frac{dC_L}{d\alpha}\right) \frac{\bar{S}}{C} \bar{C}_L \int_0^1 \left(\frac{x}{c}\right)^2 (\delta'(x) - \delta'(c))\, d\left(\frac{x}{c}\right) \qquad (4B)$$

where $\left(\frac{dC_L}{d\alpha}\right)$ is the lift curve slope of the fore-wing at the incidence when the lift coefficient of the whole wing is $\bar{C}_L$. Evaluating this expression it was found that

$$\Delta C_M = 0{\cdot}0011 \left(\frac{dC_L}{d\alpha}\right) \bar{C}_L \ . \qquad (5B)$$

Appendix C

STING BAR AND BALANCE DEFLECTION CORRECTIONS

When the wing was tested at the larger angles of incidence the sting bar and the strain-gauge balance deflected appreciably due to the aerodynamic forces on the two parts of the wing. Consequently a correction must be calculated and applied to the measured values of incidence.

The measurements of normal force and pitching moment on the fore-wing, both with and without the rear-wing fitted behind it, revealed the relative magnitudes of the aerodynamic forces on the two parts of the wing and the lines of action of these forces. The ratio of the forces on the fore-wing and rear-wing was found to be approximately 1:2. When the fore-wing and rear-wing were detached from the strain-gauge balance and the sting bar, weights were hung on the balance and the bar in the appropriate positions. It was found that the deflection of the balance was

$$\Delta\alpha = 2{\cdot}6 \text{ minutes/lb force on the balance}$$

$$= 2{\cdot}6\ q\,S\,C_N \text{ minutes} \qquad (1C)$$

where S is the area of the fore-wing and C_N is the coefficient of normal force on the fore-wing measured with the rear-wing fitted, i.e. with the fore-wing in an almost conical flow field. At the usual tunnel speed of 120 ft/sec the incidence correction is

$$\Delta\alpha = 0{\cdot}0059\ C_N \text{/radians.} \qquad (2C)$$

Table 1

RESULTS OF TESTS ON WING $\frac{\pi}{6}/0$

α deg.	$(C_N)_1$	$(C_M)_1$	$\left(\frac{C_M}{C_N}\right)_1$	C_{N_c}	$\frac{C_{N_c}}{\alpha}$
0·20	0·0053	0·0010	0·196	0·0054	1·534
0·71	0·0159	0·0032	0·203	0·0161	1·295
1·23	0·0251	0·0051	0·202	0·0254	1·183
1·73	0·0357	0·0075	0·209	0·0361	1·197
2·24	0·0489	0·0100	0·206	0·0495	1·265
2·76	0·0608	0·0126	0·207	0·0615	1·276
3·27	0·0753	0·0154	0·205	0·0762	1·334
3·79	0·0898	0·0185	0·206	0·0909	1·374
4·30	0·1057	0·0216	0·207	0·1070	1·425
4·81	0·1216	0·0249	0·205	0·1231	1·465
5·37	0·1388	0·0284	0·206	0·1405	1·498
6·40	0·1745	0·0358	0·207	0·1766	1·580
7·45	0·2120	0·0432	0·206	0·2145	1·647
8·48	0·2540	0·0516	0·205	0·2570	1·738
9·52	0·2960	0·0604	0·206	0·2996	1·800
10·61	0·3430	0·0700	0·206	0·3471	1·877
11·65	0·3940	0·0800	0·205	0·3987	1·962
12·69	0·4440	0·0906	0·207	0·4493	2·029
13·74	0·4980	0·1013	0·206	0·5040	2·101
14·79	0·5540	0·1133	0·207	0·5606	2·171
15·84	0·6120	0·1249	0·207	0·6193	2·240
0·20	0·0053	0·0010	0·196	0·0054	1·533
-0·30	-0·0066	-0·0011	0·172	-0·0067	1·283
-0·81	-0·0145	-0·0031	0·214	-0·0147	1·039
-1·33	-0·0251	-0·0051	0·202	-0·0254	1·095
-1·83	-0·0370	-0·0076	0·203	-0·0374	1·173
-2·34	-0·0502	-0·0103	0·207	-0·0508	1·243
-2·86	-0·0635	-0·0128	0·201	-0·0643	1·287
-3·37	-0·0780	-0·0135	0·173	-0·0789	1·342
-3·89	-0·0925	-0·0189	0·204	-0·0936	1·379
-4·40	-0·1084	-0·0220	0·205	-0·1097	1·428
-4·91	-0·1243	-0·0253	0·204	-0·1258	1·476

Table 1 (Contd)

Increased sensitivity tests

α deg.	$(C_N)_1$	C_{N_c}	$\frac{C_{N_c}}{\alpha}$
0·02	0·0004	0·0004	1·012
0·23	0·0043	0·0044	1·088
0·51	0·0097	0·0098	1·103
0·76	0·0145	0·0147	1·107
1·00	0·0198	0·0200	1·145
1·28	0·0259	0·0262	1·175
1·53	0·0313	0·0317	1·186
1·80	0·0380	0·0385	1·225
2·06	0·0444	0·0449	1·248
2·31	0·0510	0·0516	1·280
2·58	0·0577	0·0583	1·294
2·83	0·0642	0·0648	1·340
3·08	0·0707	0·0716	1·330
2·90	0·0662	0·0670	1·324
2·64	0·0595	0·0602	1·307
2·37	0·0524	0·0530	1·281
2·11	0·0459	0·0465	1·262
1·85	0·0394	0·0399	1·235
1·59	0·0332	0·0336	1·208
1·33	0·0271	0·0274	1·182
1·08	0·0219	0·0222	1·173
0·82	0·0162	0·0164	1·147
0·55	0·0106	0·0107	1·117
0·30	0·0056	0·0057	1·090
0·05	0·0011	0·0011	1·237
-0·22	-0·0041	-0·0042	1·092
-0·47	-0·0090	-0·0091	1·111
-0·73	-0·0142	-0·0144	1·131
-0·98	-0·0196	-0·0198	1·160
-1·24	-0·0252	-0·0255	1·175
-1·51	-0·0315	-0·0319	1·207
-1·76	-0·0374	-0·0379	1·233
-2·04	-0·0442	-0·0447	1·257
-2·29	-0·0504	-0·0510	1·275
-2·55	-0·0570	-0·0577	1·296
-2·80	-0·0637	-0·0645	1·319
-3·07	-0·0712	-0·0721	1·344
2·86	-0·0644	-0·0651	1·305
2·60	-0·0577	-0·0583	1·285
2·33	-0·0510	-0·0516	1·269
2·08	-0·0446	-0·0451	1·244
1·82	-0·0378	-0·0383	1·203
1·55	-0·0318	-0·0322	1·187
1·37	-0·0259	-0·0262	1·145
1·04	-0·0203	-0·0205	1·128
0·78	-0·0148	-0·0150	1·101
0·52	-0·0101	-0·0102	1·123
0·28	-0·0052	-0·0053	1·074
0·01	-0·0002	-0·0002	1·012

Table 2

RESULTS OF TESTS ON WING $\frac{\pi}{3}/0$

α deg.	$(C_N)_1$	$(C_M)_1$	$\left(\frac{C_M}{C_N}\right)_1$	C_{N_c}	$\frac{C_{N_c}}{\alpha}$
0·20	0·0039	0·0008	0·210	0·0039	1·140
0·71	0·0131	0·0026	0·198	0·0132	1·059
1·22	0·0222	0·0045	0·201	0·0223	1·046
1·73	0·0313	0·0063	0·202	0·0314	1·041
2·24	0·0418	0·0084	0·201	0·0420	1·073
2·76	0·0522	0·0106	0·203	0·0524	1·087
3·32	0·0652	0·0133	0·203	0·0655	1·132
3·82	0·0770	0·0155	0·201	0·0773	1·160
4·34	0·0900	0·0181	0·200	0·0904	1·194
4·85	0·1044	0·0204	0·196	0·1048	1·238
5·37	0·1174	0·0233	0·199	0·1179	1·258
6·40	0·1447	0·0289	0·200	0·1453	1·301
7·43	0·1748	0·0352	0·201	0·1755	1·353
8·47	0·2075	0·0415	0·200	0·2083	1·409
9·50	0·2435	0·0483	0·198	0·2443	1·470
10·59	0·2832	0·0563	0·200	0·2844	1·538
11·63	0·3209	0·0641	0·200	0·3221	1·585
12·68	0·3639	0·0726	0·200	0·3654	1·648
13·72	0·4095	0·0816	0·200	0·4113	1·714
14·83	0·4592	0·0919	0·201	0·4615	1·779
15·87	0·5081	0·1018	0·200	0·5107	1·842
+0·20	0·0039	0·0008	0·205	0·0039	1·135
−0·30	−0·0039	−0·0004	0·102	−0·0039	0·756
−0·81	−0·0143	−0·0027	0·188	−0·0144	1·016
−1·32	−0·0260	−0·0049	0·187	−0·0261	1·136
−1·83	−0·0339	−0·0062	0·184	−0·0340	1·066
−2·34	−0·0444	−0·0081	0·182	−0·0446	1·091
−2·86	−0·0561	−0·0107	0·190	−0·0563	1·129
−3·37	−0·0665	−0·0130	0·195	−0·0668	1·136
−3·87	−0·0783	−0·0154	0·196	−0·0786	1·165
−4·39	−0·0914	−0·0178	0·195	−0·0918	1·198
−4·90	−0·1044	−0·0202	0·194	−0·1048	1·225

Table 2 (Contd)

Increased sensitivity tests

α deg.	$(C_N)_1$	C_{N_c}	$\frac{C_{N_c}}{\alpha}$
-0·34	-0·0065	-0·0065	1·106
-0·09	-0·0018	-0·0018	1·129
+0·16	0·0029	0·0029	1·040
0·41	0·0072	0·0072	1·004
0·66	0·0114	0·0115	0·995
1·18	0·0213	0·0214	1·038
1·69	0·0308	0·0309	1·048
2·20	0·0412	0·0414	1·075
2·72	0·0524	0·0526	1·107
2·24	0·0420	0·0422	1·078
1·73	0·0317	0·0318	1·054
1·23	0·0210	0·0211	0·981
0·71	0·0125	0·0126	1·012
0·45	0·0080	0·0080	1·017
0·20	0·0036	0·0036	1·033
-0·30	-0·0049	-0·0049	0·946
-0·55	-0·0096	-0·0096	1·044
-0·81	-0·0145	-0·0146	1·032
-1·06	-0·0192	-0·0193	1·042
-1·33	-0·0236	-0·0237	1·021
-1·83	-0·0333	-0·0334	1·048
-2·34	-0·0440	-0·0442	1·082
-2·87	-0·0548	-0·0550	1·100
-2·90	-0·0551	-0·0553	1·093
-2·38	-0·0440	-0·0442	1·064
-1·87	-0·0336	-0·0337	1·035
-1·37	-0·0245	-0·0246	1·029
-1·10	-0·0200	-0·0201	1·046
-0·85	-0·0153	-0·0154	1·038
-0·59	-0·0101	-0·0101	0·985
-0·34	-0·0065	-0·0065	1·106

Table 3

RESULTS OF TESTS ON WING $\frac{\pi}{2}/0$

α deg.	$(C_N)_1$	$(C_M)_1$	$\left(\frac{C_M}{C_N}\right)_1$	C_{N_c}	$\frac{C_{N_c}}{\alpha}$
0·23	0·0042	0·00050	0·120	0·0042	1·060
0·74	0·0113	0·00198	0·176	0·0114	0·884
1·25	0·0190	0·00347	0·183	0·0192	0·880
2·31	0·0361	0·00669	0·185	0·0365	0·907
3·33	0·0539	0·01015	0·189	0·0544	0·937
4·35	0·0734	0·01376	0·187	0·0741	0·976
5·37	0·0930	0·01762	0·189	0·0939	1·002
6·39	0·1149	0·02159	0·188	0·1160	1·041
7·46	0·1381	0·02607	0·189	0·1395	1·071
8·48	0·1623	0·03068	0·189	0·1639	1.108
9·50	0·1884	0·03528	0·187	0·1903	1·147
10·58	0·2156	0·04051	0·188	0·2178	1·178
11·61	0·2447	0·04587	0·188	0·2471	1·220
12·65	0·2744	0·05148	0·188	0·2771	1·255
13·71	0·3063	0·05770	0·189	0·3094	1·292
14·74	0·3389	0·06420	0·189	0·3423	1·330
15·77	0·3721	0·07060	0·190	0·3758	1·365
0·23	0·0035	0·00037	0·106	0·0035	0·883
-0·27	-0·0042	-0·00115	0·275	-0·0042	0·902
-0·78	-0·0119	-0·00088	0·074	-0·0120	0·890
-1·80	-0·0273	-0·00570	0·209	-0·0276	0·877
-2·81	-0·0444	-0·00905	0·204	-0·0448	0·914
-3·83	-0·0616	-0·01240	0·201	-0·0622	0·931
-4·85	-0·0830	0·01637	0·197	-0·0838	0·989

Table 3 (Contd)

Increased sensitivity tests

α deg.	$(C_N)_1$	C_{N_c}	$\frac{C_{N_c}}{\alpha}$
0·25	0·0039	0·0039	0·914
0·53	0·0074	0·0074	0·808
0·79	0·0123	0·0124	0·905
1·02	0·0153	0·0155	0·869
1·51	0·0232	0·0234	0·886
2·03	0·0316	0·0319	0·900
2·54	0·0405	0·0409	0·923
3·04	0·0489	0·0494	0·921
2·05	0·0340	0·0343	0·960
1·02	0·0158	0·0160	0·896
0·76	0·0118	0·0119	0·905
0·52	0·0079	0·0080	0·879
0·24	0·0039	0·0039	0·949
−0·25	0·0034	0·0034	0·801
−0·52	0·0083	0·0084	0·931
−1·02	0·0158	0·0160	0·896
−1·54	0·0237	0·0239	0·891
−2·03	0·0316	0·0319	0·900
−1·53	0·0242	0·0244	0·915
−1·04	0·0163	0·0165	0·907
−0·49	0·0079	0·0080	0·932
−0·25	0·0044	0·0045	1·030

Table 4

RESULTS OF TESTS ON WING $\frac{2\pi}{3}$/O

α deg.	$(C_N)_1$	$(C_M)_1$	$\left(\frac{C_M}{C_N}\right)_1$	C_{N_c}	$\frac{C_{N_c}}{\alpha}$
0·36	0·0025	0·00036	0·146	0·0025	0·398
1·37	0·0123	0·00199	0·161	0·0124	0·516
2·38	0·0202	0·00399	0·197	0·0203	0·488
3·44	0·0300	0·00580	0·193	0·0301	0·502
4·46	0·0389	0·00751	0·193	0·0390	0·502
5·46	0·0476	0·00929	0·195	0·0478	0·501
6·48	0·0597	0·01120	0·188	0·0599	0·53C
7·49	0·0709	0·01319	0·186	0·0712	0·544
8·50	0·0831	0·01544	0·186	0·0834	0·562
9·52	0·0966	0·01779	0·184	0·0970	0·583
10·58	0·1110	0·02068	0·186	0·1115	0·603
11·60	0·1240	0·02327	0·187	0·1245	0·614
12·62	0·1385	0·02646	0·191	0·1390	0·631
13·64	0·1557	0·02984	0·192	0·1563	0·656
14·76	0·1735	0·03284	0·189	0·1742	0·676
15·73	0·1905	0·03598	0·189	0·1913	0·696
0·36	0·0033	0·00046	0·138	0·0033	0·525
-0·64	-0·0057	-0·00114	0·200	-0·0057	0·510
-1·66	-0·0145	-0·00277	0·191	-0·0146	0·502
-2·67	-0·0235	-0·00439	0·186	-0·0236	0·506
-3·67	-0·0324	-0·00619	0·191	-0·0325	0·507
-4·69	-0·0413	-0·00799	0·194	-0·0415	0·506

Table 4 (Contd)

Increased sensitivity tests

α deg.	$(C_N)_1$	C_{N_c}	$\frac{C_{N_c}}{\alpha}$
-1·90	-0·0162	-0·0162	0·490
-1·63	-0·0142	-0·0143	0·502
-1·40	-0·0123	-0·0124	0·508
-1·15	-0·0100	-0·0100	0·500
-0·90	-0·0077	-0·0077	0·492
-0·65	-0·0057	-0·0058	0·509
-0·40	-0·0034	-0·0034	0·477
-0·15	-0·0011	-0·0011	0·448
0·11	+0·0007	+0·0007	0·406
0·35	+0·0030	+0·0030	0·506
0·60	0·0050	0·0050	0·479
0·85	0·0073	0·0073	0·496
1·10	0·0092	0·0092	0·483
1·37	0·0119	0·0120	0·502
1·61	0·0135	0·0135	0·482
1·87	0·0153	0·0153	0·471
2·38	0·0204	0·0204	0·493
2·89	0·0251	0·0252	0·500
3·39	0·0292	0·0293	0·495
3·89	0·0339	0·0340	0·501
4·41	0·0393	0·0395	0·512
4·91	0·0436	0·0438	0·510
5·91	0·0532	0·0534	0·517
6·93	0·0636	0·0639	0·527
7·95	0·0759	0·0762	0·549
8·95	0·0882	0·0886	0·567
9·96	0·1013	0·1017	0·585
10·97	0·1150	0·1155	0·602
11·99	0·1305	0·1310	0·626
13·01	0·1460	0·1466	0·645
14·02	0·1625	0·1632	0·666
15·04	0·1790	0·1797	0·684

Table 5

EFFECT OF THE SPANWISE GAP ON THE AERODYNAMIC NORMAL FORCE ON THE WINGS

Wing	α	δ_3	C_N at $\delta = \delta_3$	δ_2	C_N at $\delta = \delta_2$	δ_1	C_N at $\delta = \delta_1$	$\frac{\delta_1}{(C_N)_1}\left(\frac{dC_N}{d\delta}\right)_1$
$\frac{\pi}{6}/0$	10·61	0·066	0·333	0·041	0·338	0·016	0·343	0·012
	11·65		0·382		0·386		0·394	
	12·69		0·430		0·438		0·444	
	13·74		0·483		0·492		0·498	
	14·79		0·539		0·545		0·554	
	15·84		0·594		0·605		0·612	
$\frac{\pi}{3}/0$	10·59	0·051	0·274	0·030	0·278	0·005	0·283	0·004
	11·63		0·311		0·316		0·321	
	12·68		0·352		0·357		0·363	
	13·72		0·397		0·402		0·409	
	14·83		0·447		0·452		0·459	
	15·87		0·496		0·502		0·508	
$\frac{\pi}{2}/0$	10·58	0·260	0·193	0·110	0·204	0·013	0·216	0·010
	11·61		0·220		0·233		0·245	
	12·65		0·249		0·260		0·274	
	13·71		0·277		0·289		0·306	
	14·74		0·307		0·319		0·339	
	15·77		0·339		0·352		0·372	
$\frac{2\pi}{3}/0$	10·56	0·057	0·105	0·029	0·109	0·005	0·111	0·004
	11·57		0·118		0·122		0·124	
	12·59		0·134		0·137		0·139	
	13·60		0·151		0·153		0·156	
	14·67		0·168		0·170		0·173	
	15·68		0·184		0·187		0·190	

Table 6

RESULTS OF EXPERIMENT

Wing	$\frac{\pi}{6}/0$	$\frac{\pi}{3}/0$	$\frac{\pi}{2}/0$	$\frac{2\pi}{3}/0$
Aspect ratio	0·8	0·8	0·8	0·462
a_{th}	0·906	0·828	0·756	0·695
a_{ex}/a_{th}	0·945	0·945	0·945	0·964
a_{ex}	0·856	0·783	0·714	0·670
$dC_{N_c}/d\alpha$ $(\alpha = 0)$	1·074	0·982	0·896	0·487
p	1·9	2·1	2·3	2·8
b	4·38	2·99	1·56	0·40

31

SYMBOLS

A	aspect ratio
a	linear normal force parameter
b	non-linear normal force parameter in main text; wind-tunnel breadth in Appendix
B	base area of wing
c	wing chord, measured along its axis of symmetry
C	wind-tunnel cross-sectional area
C_L	lift coefficient
C_M	pitching moment coefficient
C_N	normal force coefficient
C_{N_c}	normal force coefficient associated with a conical flow field
F,f	constraint effect functions
K	cotangent of the leading-edge sweepback angle
m	source of sink strength
n	(leading-edge angle)/π
N	normal force
p	non-linear normal force parameter
q	wind-tunnel dynamic pressure
S	area bounded by leading-edges and rear of fore-wing
U	velocity of wind-tunnel free stream
ΔU	velocity increment
x,y,z	orthogonal system of axes, x measured downstream from wing apex
x'	distance from apex to the line of action of the normal force
α	angle of incidence
δ	gap width
δ_1	minimum gap width
δ_o,δ'	constraint effect functions
ϵ	total blockage correction factor
λ	wind-tunnel height/breadth ratio

List of subscripts

ex	found from experimental results
th	found from theory
unc	uncorrected
1	measured when $\delta = \delta_1$

REFERENCES

No.	Author	Title, etc
1	E. C. Maskell	Similarity laws governing the initial growth of leading-edge vortex sheets in conical flow past sharp-edged slender bodies. Xth International Congress of Applied Mechanics, Stresa, 1960
2	Robert T. Jones	Properties of low-aspect-ratio pointed wings at speeds below and above the speed of sound. N.A.C.A. T.N. No.1032. March 1946
3	R. F. Keating	Unpublished work.
4	D. J. Kettle	Description of the pitch/roll support rig installation designed for sting-mounted models in the 4 ft x 3 ft low-turbulence tunnel. R.A.E. Tech Note No. Aero 2977. 1964
5	J. R. Anderson	A Note on the use of strain gauges in wind-tunnel balances. R.A.E. Tech Note No. Aero 2290. January 1954
6	J. R. Cole S. A. Mitchell	Unpublished work.
7	Mac C. Adams	Leading-edge separation from delta wings at supersonic speeds. Journal of Aero Sciences, Vol.20, No.6 p.430, June 1953
8	R. H. Edwards	Leading edge separation from delta wings. Journal of Aero Sciences, Vol.21, No.2, p.134, February 1954
9	R. C. Pankhurst D. W. Holder	Wind-tunnel Technique, Chapter 8. Pitman's Press, London, 1948
10	E. C. Maskell	A theory of the blockage effects on bluff bodies and stalled wings in a closed wind tunnel. A.R.C. R. & M. 3400 November 1963
11	Sune B. Berndt	Wind Tunnel interference due to lift for delta wings of small aspect ratio. K.T.H. Aero TN 19. September 1950

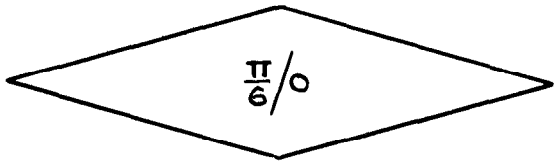

A=0·8

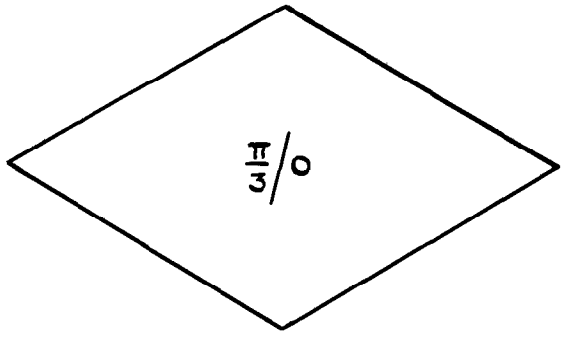

A=0·8

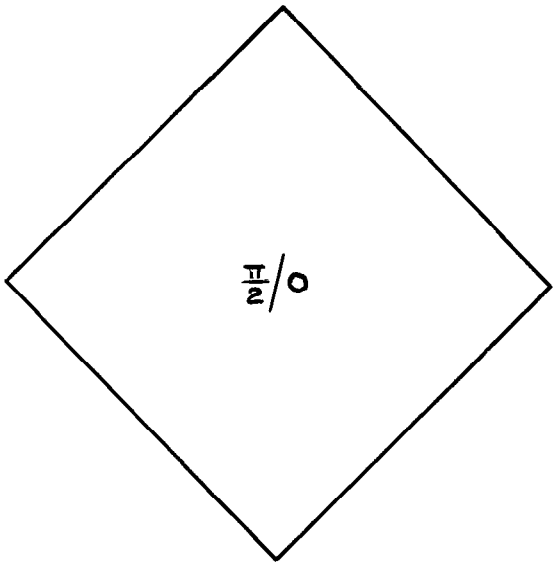

A=0·8

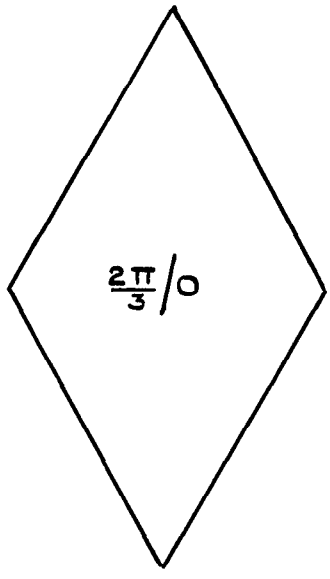

A=0·462

FIG. 1 CROSS-SECTIONAL SHAPES OF WINGS TESTED.

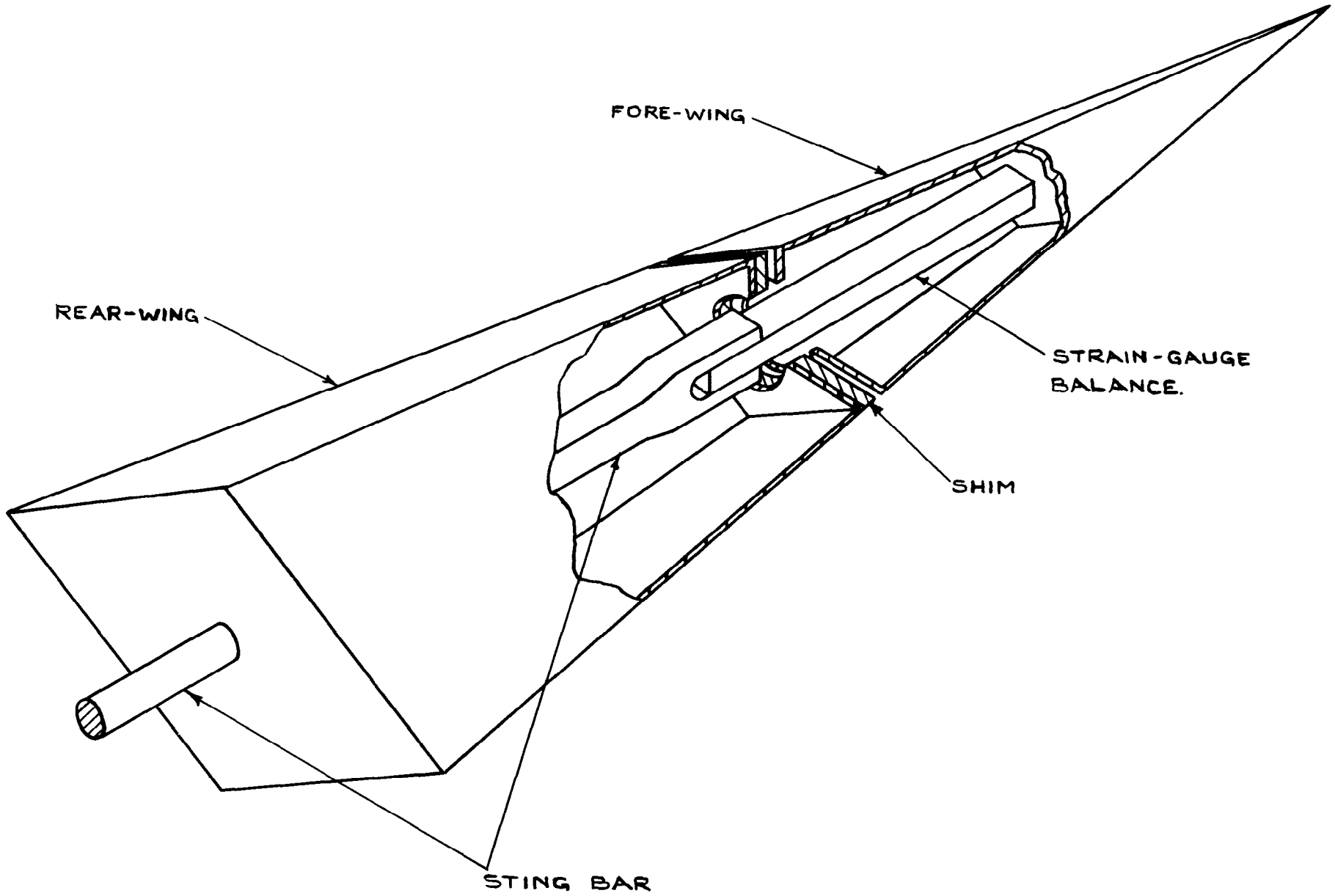

FIG. 2 REAR-WING AND FORE-WING MOUNTED ON THE STING BAR AND STRAIN-GAUGE BALANCE RESPECTIVELY

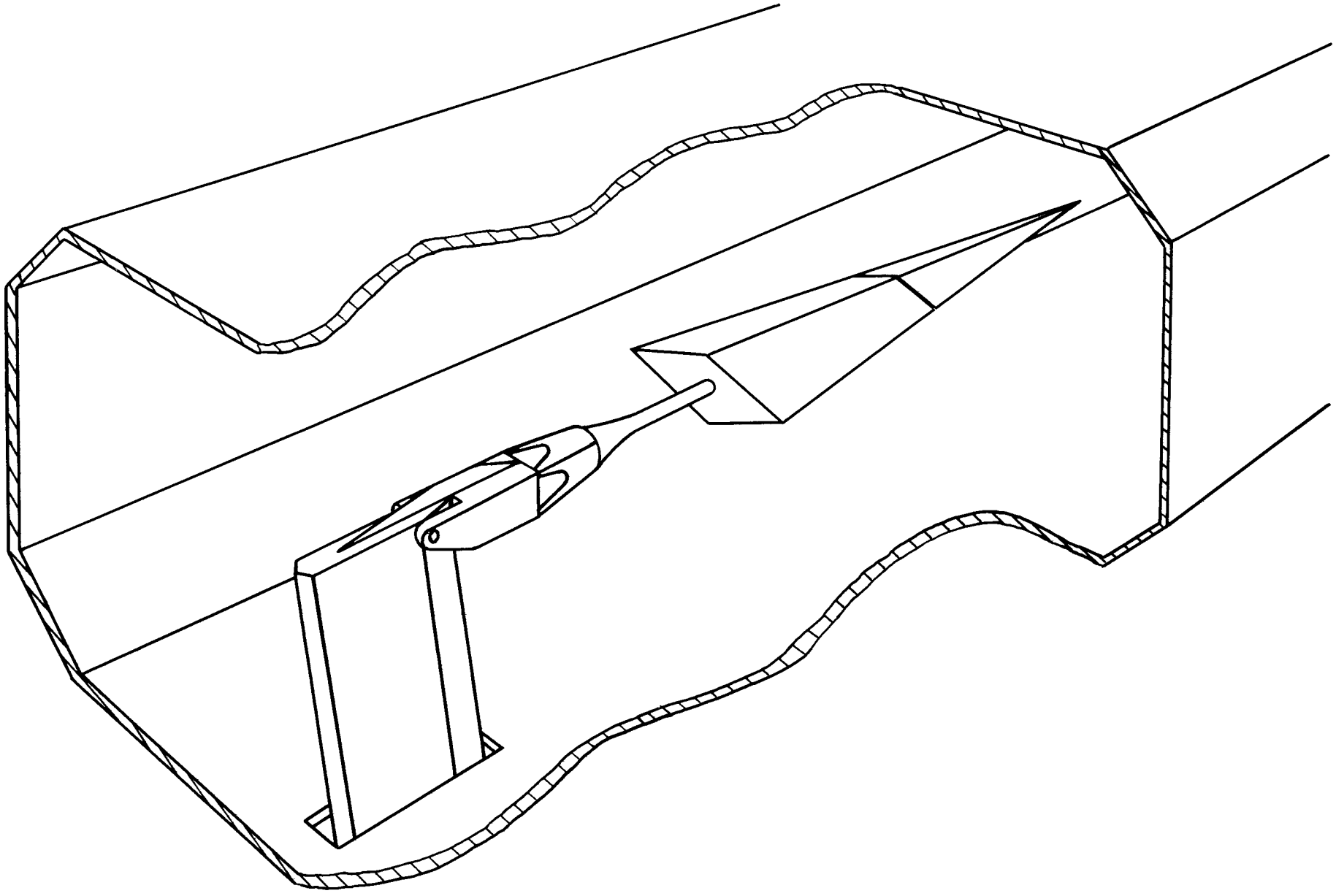

FIG.3. WING MOUNTED ON SUPPORT RIG IN 4' x 3' WING-TUNNEL.

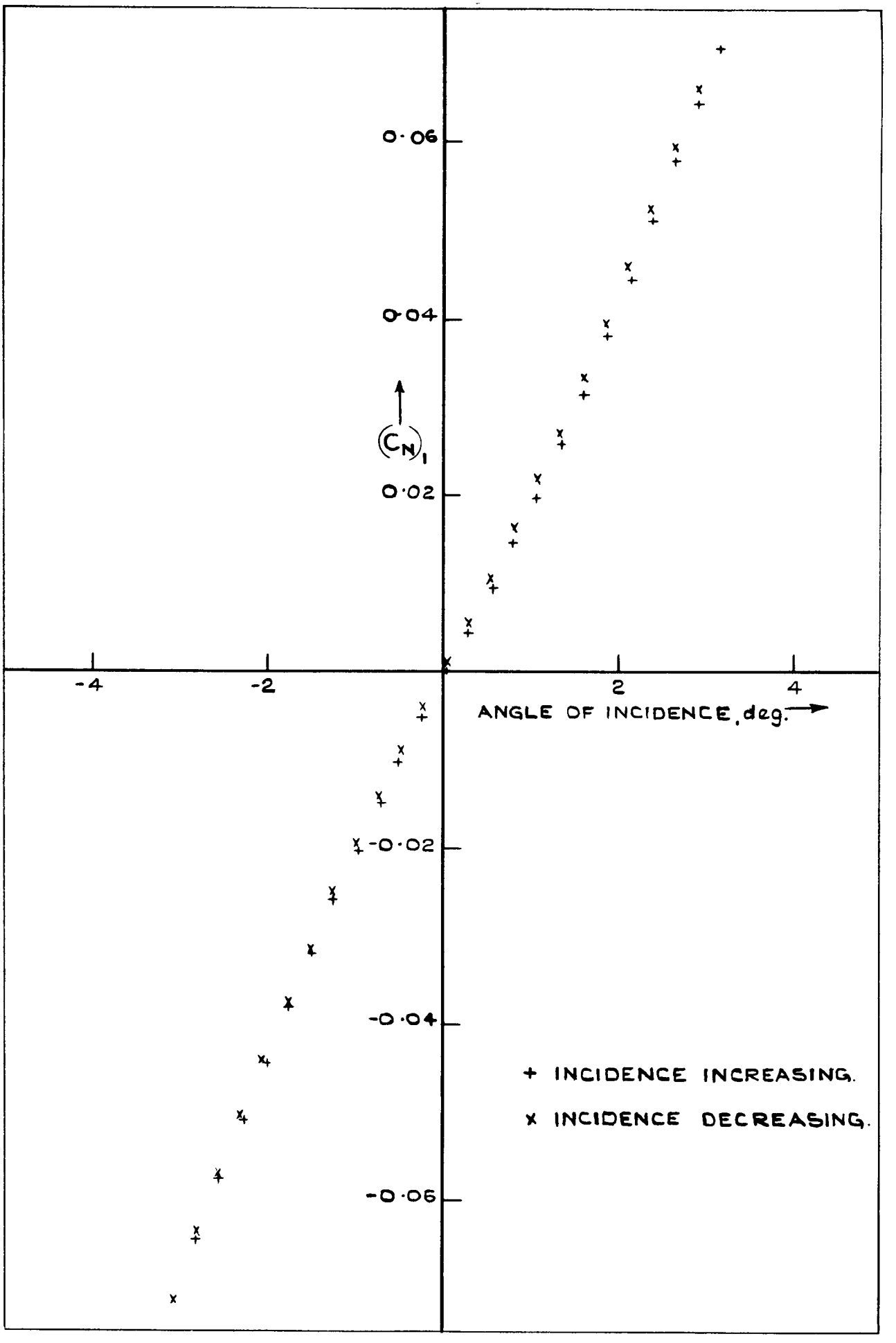

FIG. 4 NORMAL FORCE CHARACTERISTIC OF WING $\frac{\Pi}{6}/0$ MEASURED AT LOW INCIDENCE.

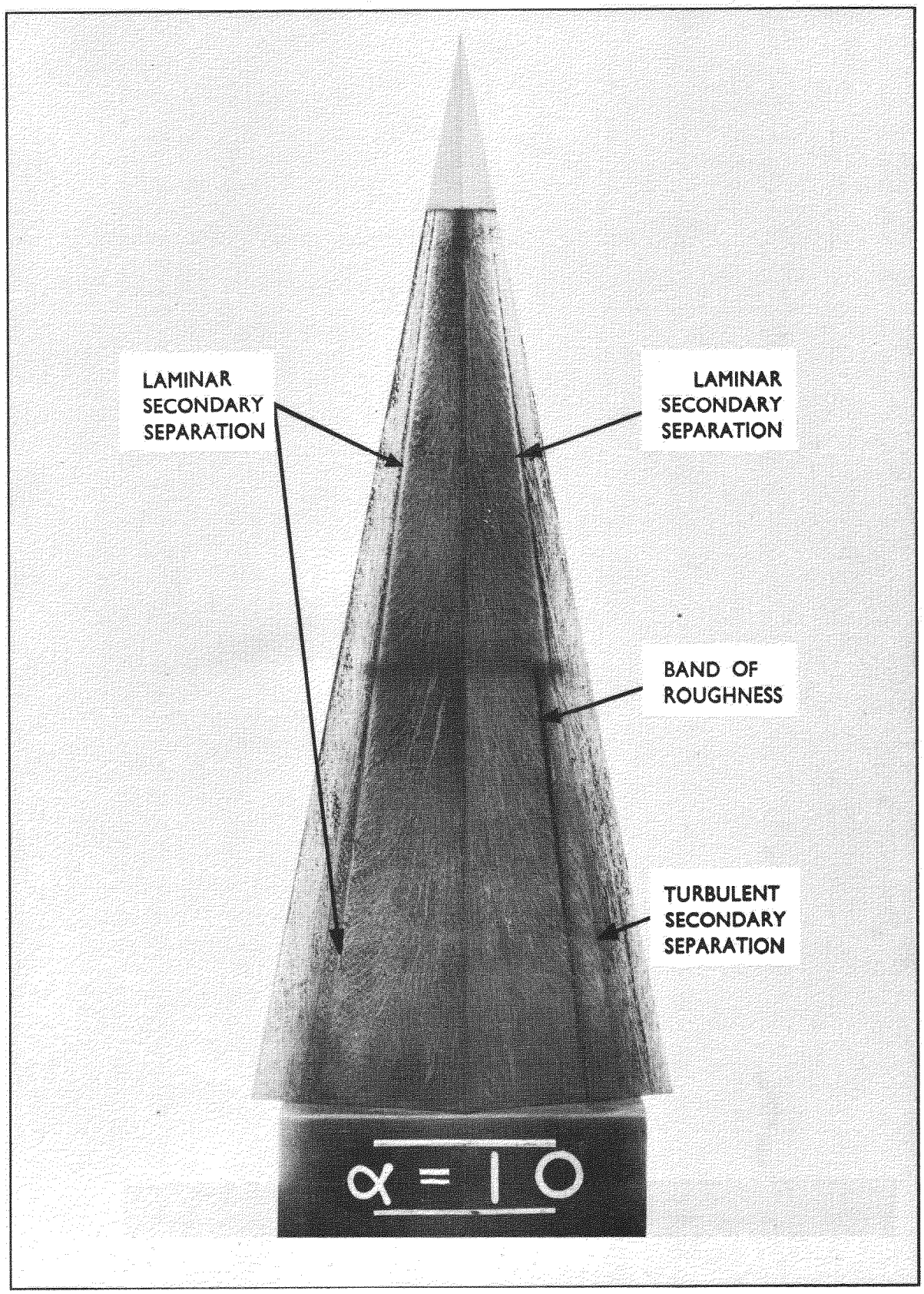

Fig.5. Surface flow pattern on the upper surface of wing $\frac{\pi}{6}/0$

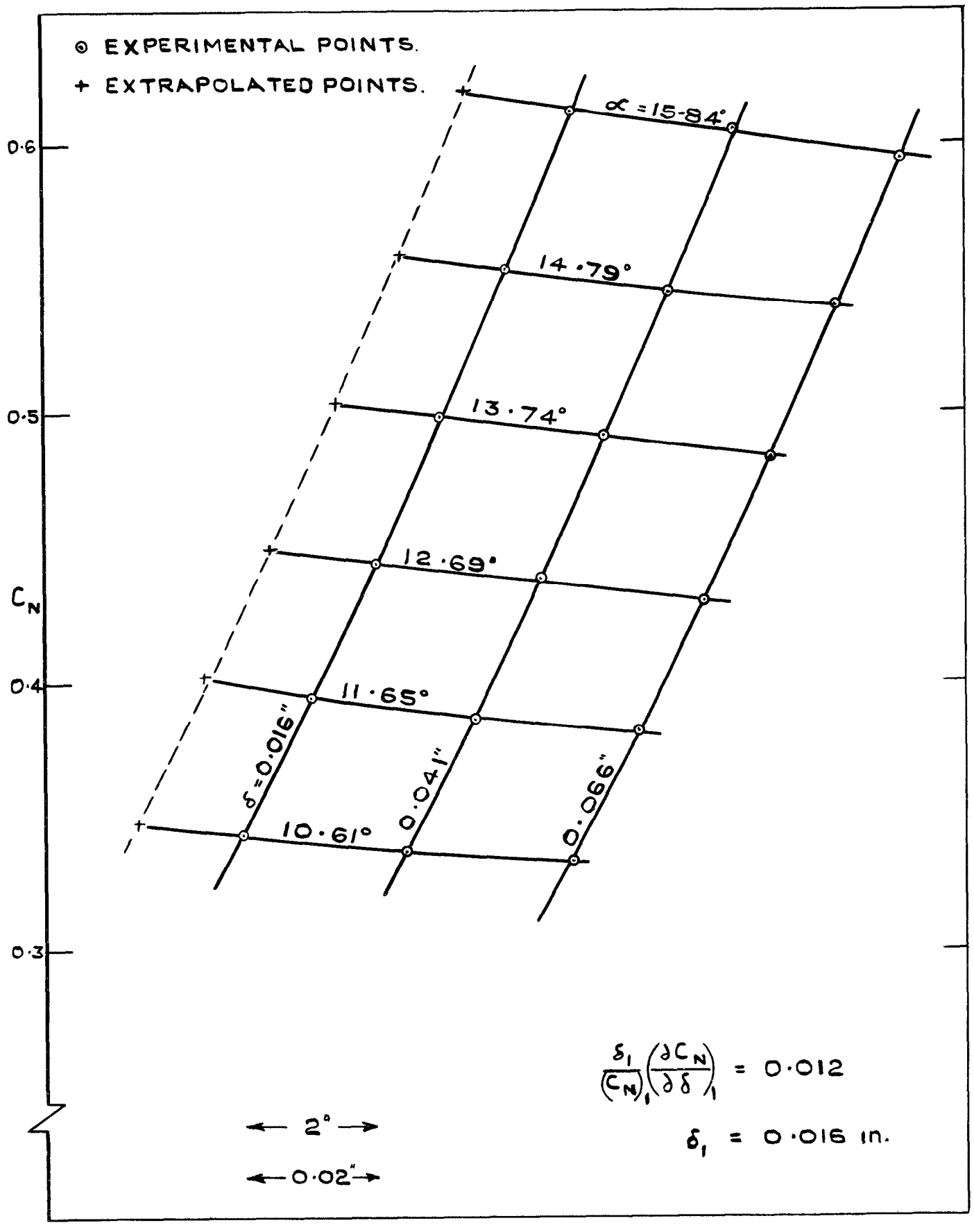

FIG. 6 @ EFFECT OF GAP ON THE NORMAL FORCE CHARACTERISTIC OF WING $\frac{\pi}{6}$/O

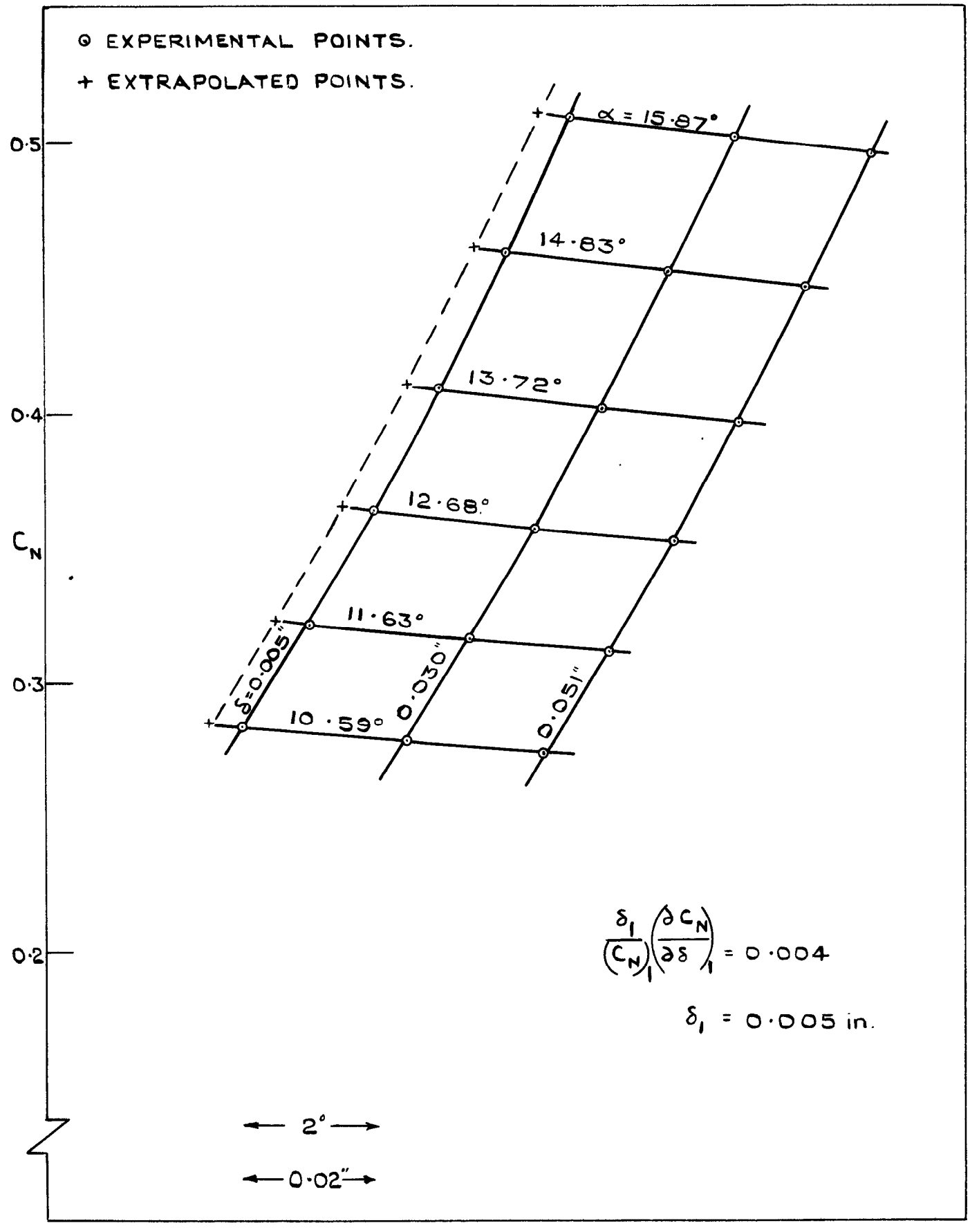

FIG.6 (b) EFFECT OF GAP ON THE NORMAL FORCE CHARACTERISTIC OF WING $\frac{\pi}{3}/0$

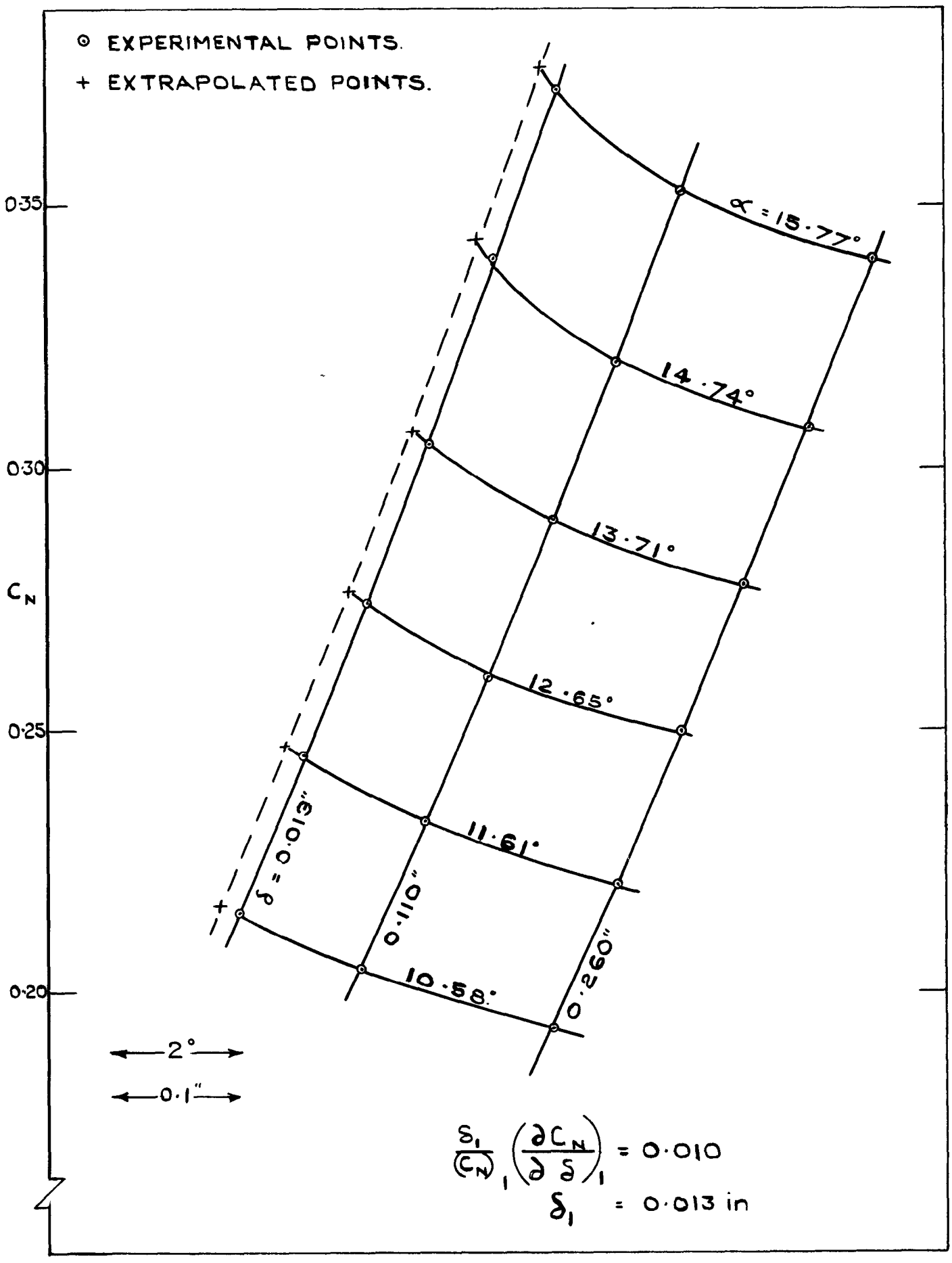

FIG 6 (c) EFFECT OF GAP ON THE NORMAL FORCE CHARACTERISTIC OF WING $\frac{\pi}{2}/0$

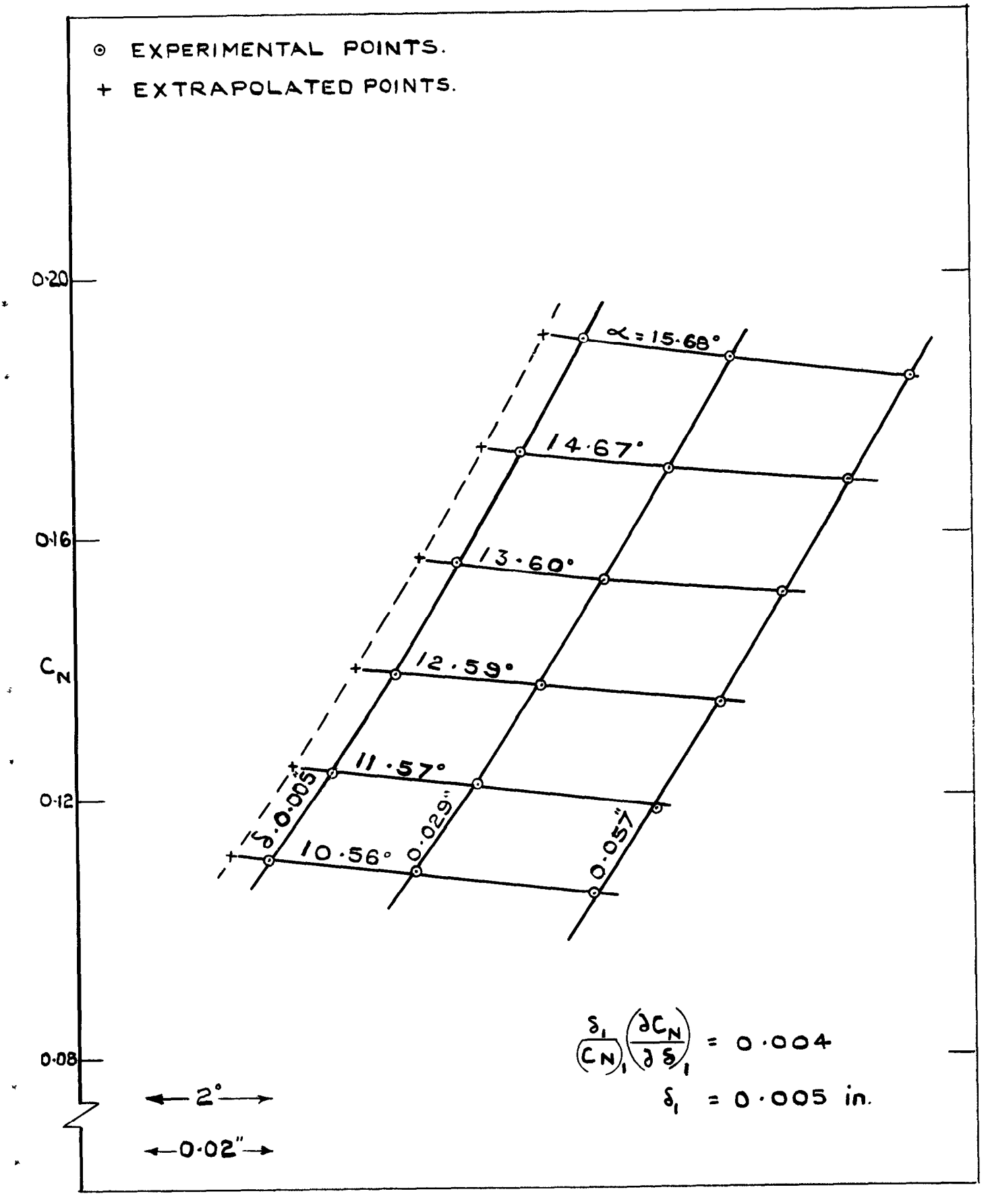

FIG. 6 (d) EFFECT OF GAP ON THE NORMAL FORCE CHARACTERISTIC OF WING $\frac{2\pi}{3}$/O

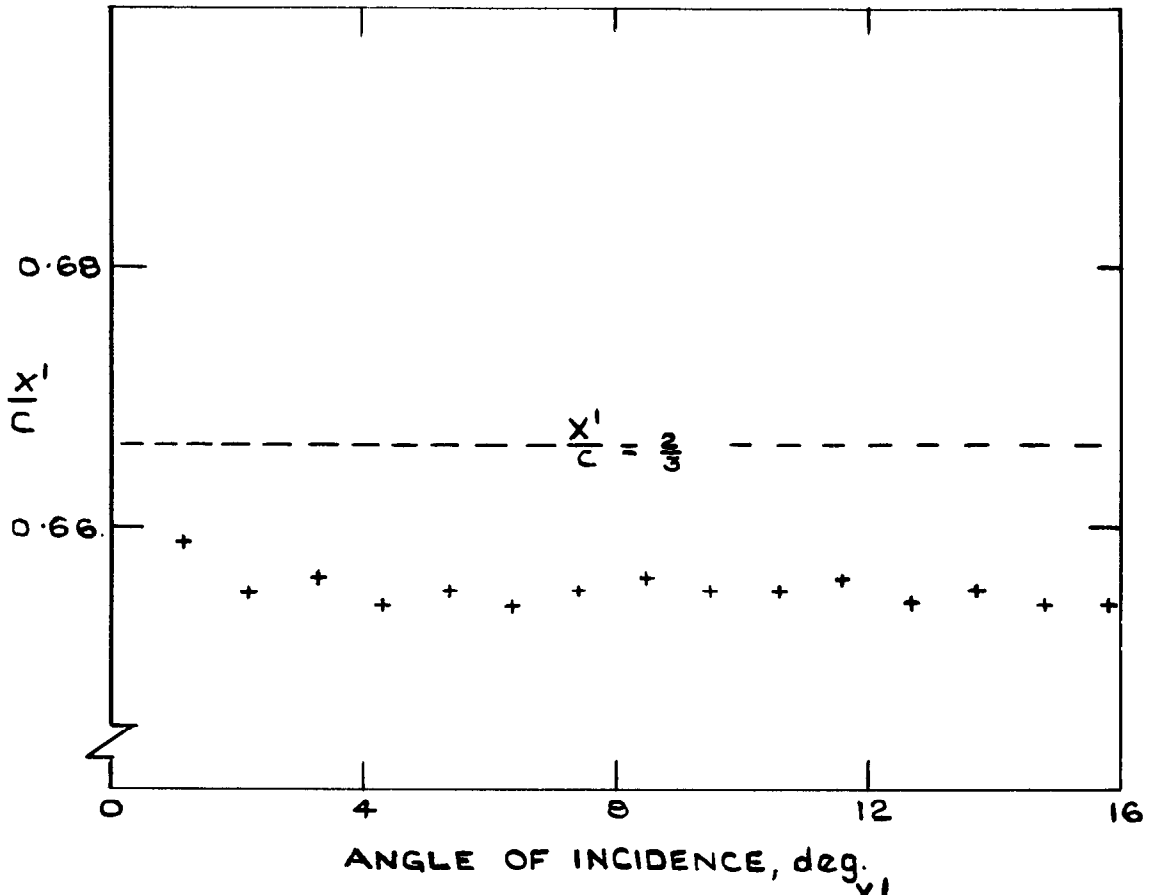

FIG.7(a) VARIATION WITH INCIDENCE OF $\frac{x'}{c}$ FOR WING $\frac{\pi}{6}/0$
$\delta_1 = 0 \cdot 016$ in.

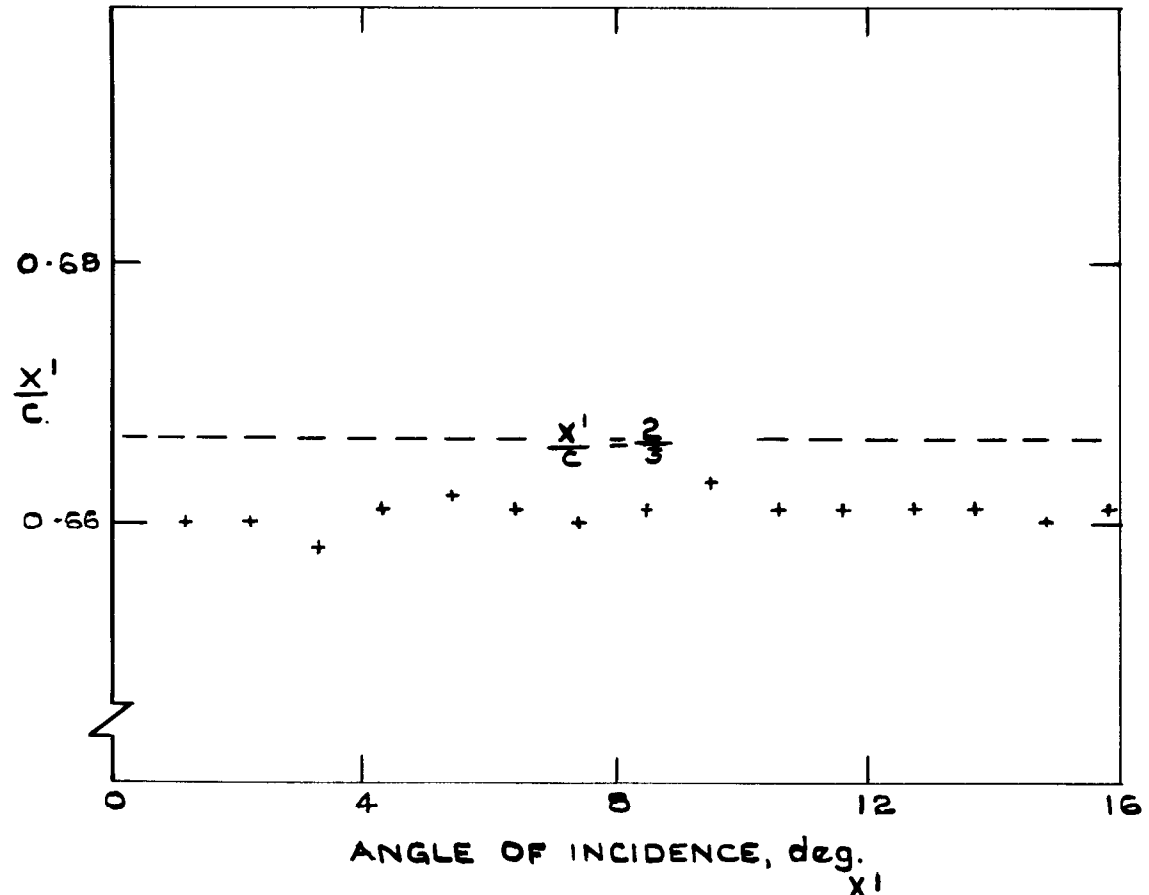

FIG.7(b) VARIATION WITH INCIDENCE OF $\frac{x'}{c}$ FOR WING $\frac{\pi}{3}/0$
$\delta_1 = 0 \cdot 005$ in.

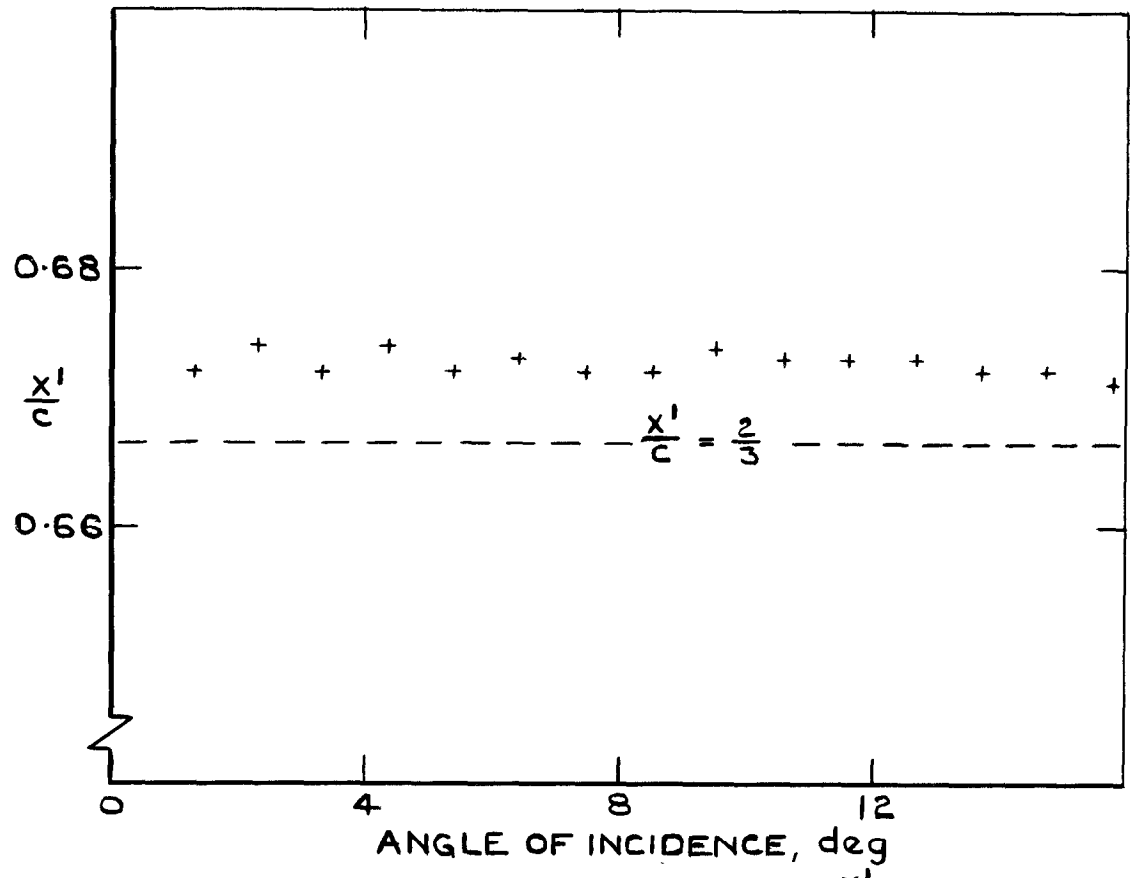

FIG. 7 (c) VARIATION WITH INCIDENCE OF $\frac{x'}{c}$ FOR WING $\frac{\pi}{2}/0$

$\delta_1 = 0 \cdot 013$ in.

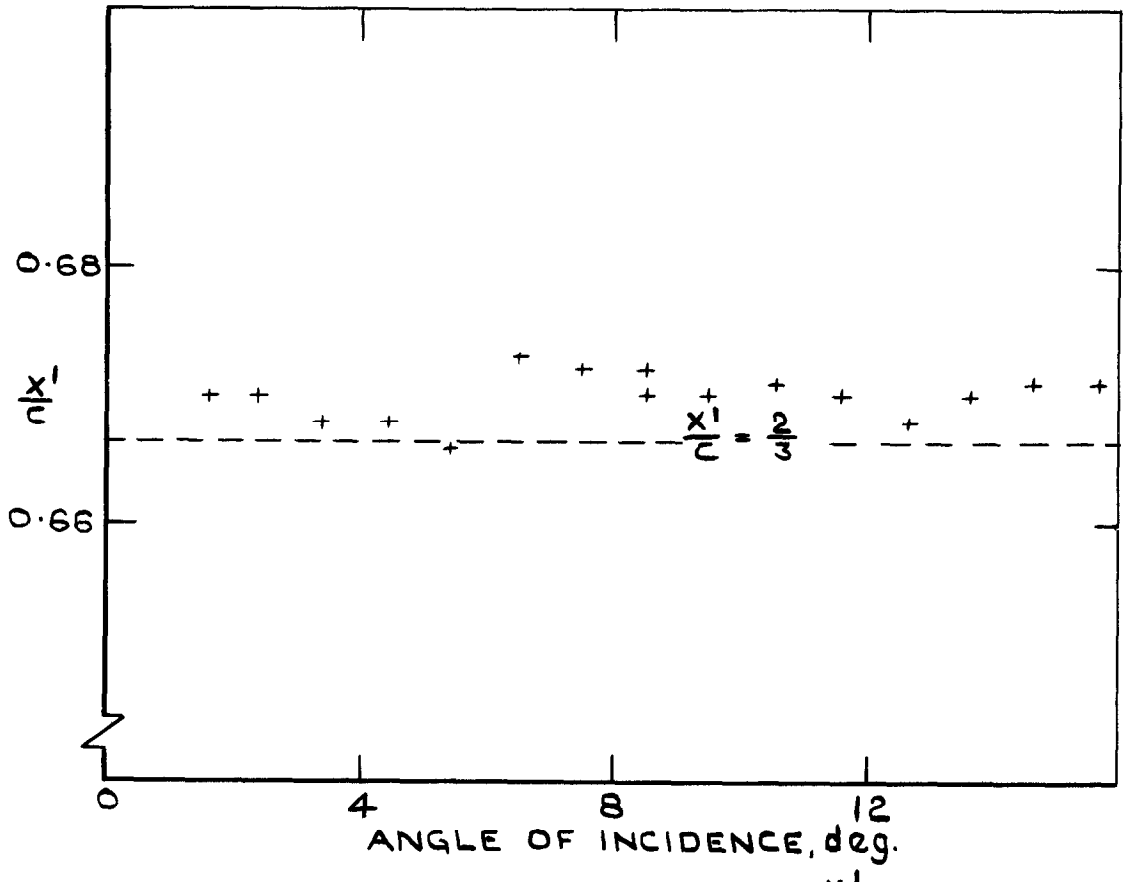

FIG. 7 (d) VARIATION WITH INCIDENCE OF $\frac{x'}{c}$ FOR WING $\frac{2\pi}{3}/0$

$\delta_1 = 0 \cdot 005$ in.

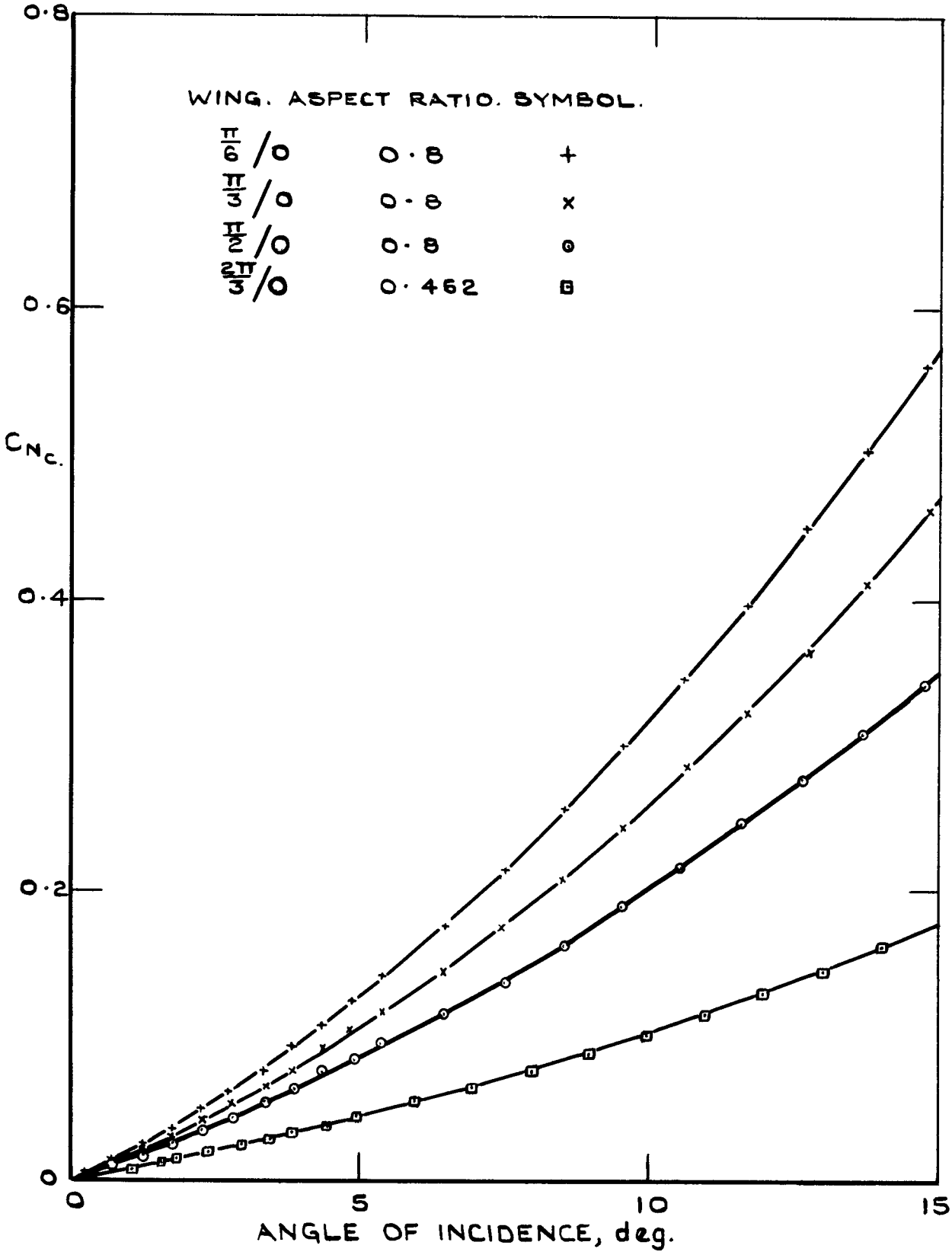

FIG 8 NORMAL FORCE CHARACTERISTICS OF FOUR SLENDER WINGS IN CONICAL FLOW.

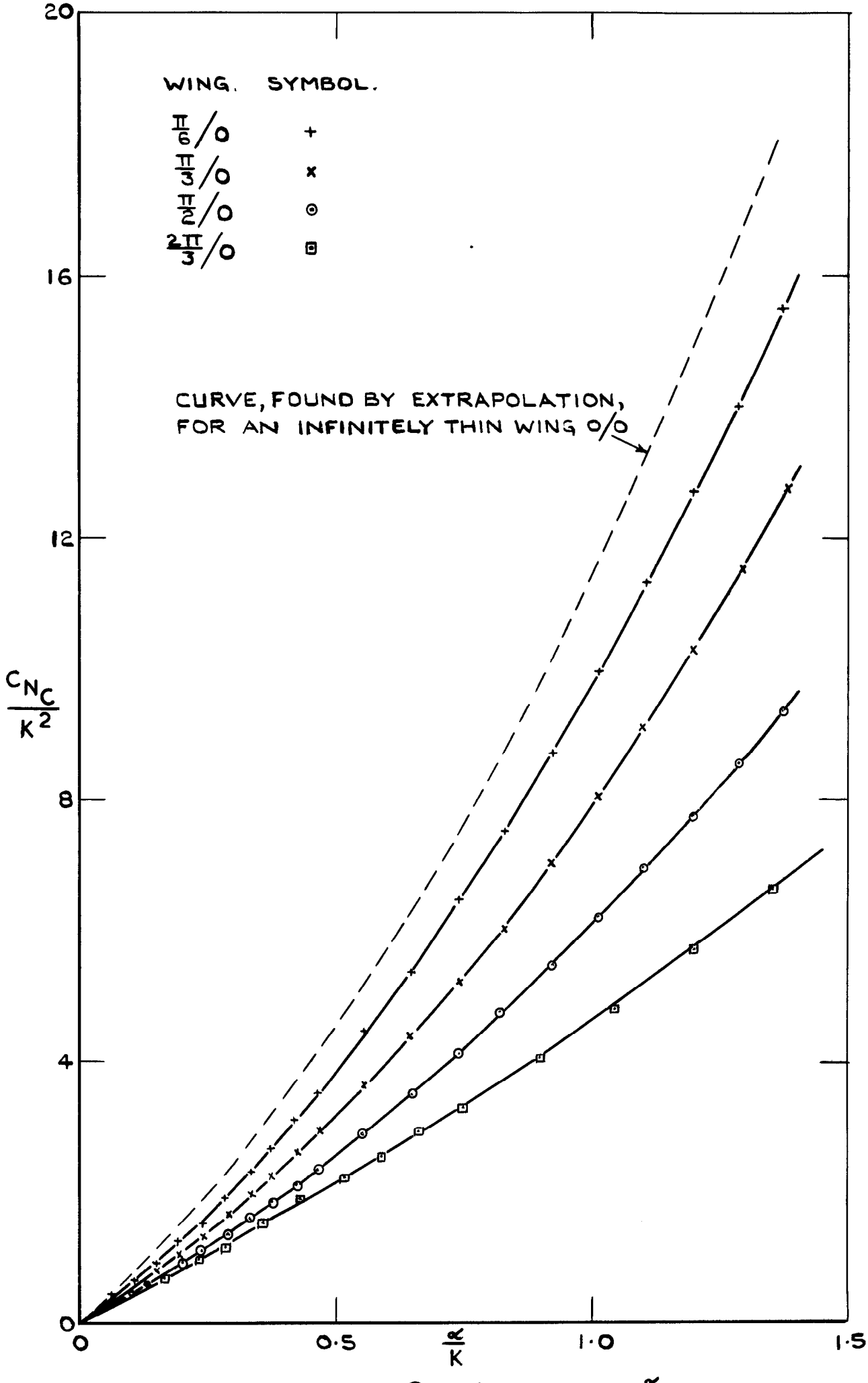

FIG. 9. VARIATION OF C_{N_C}/K^2 WITH $\frac{\alpha}{K}$.

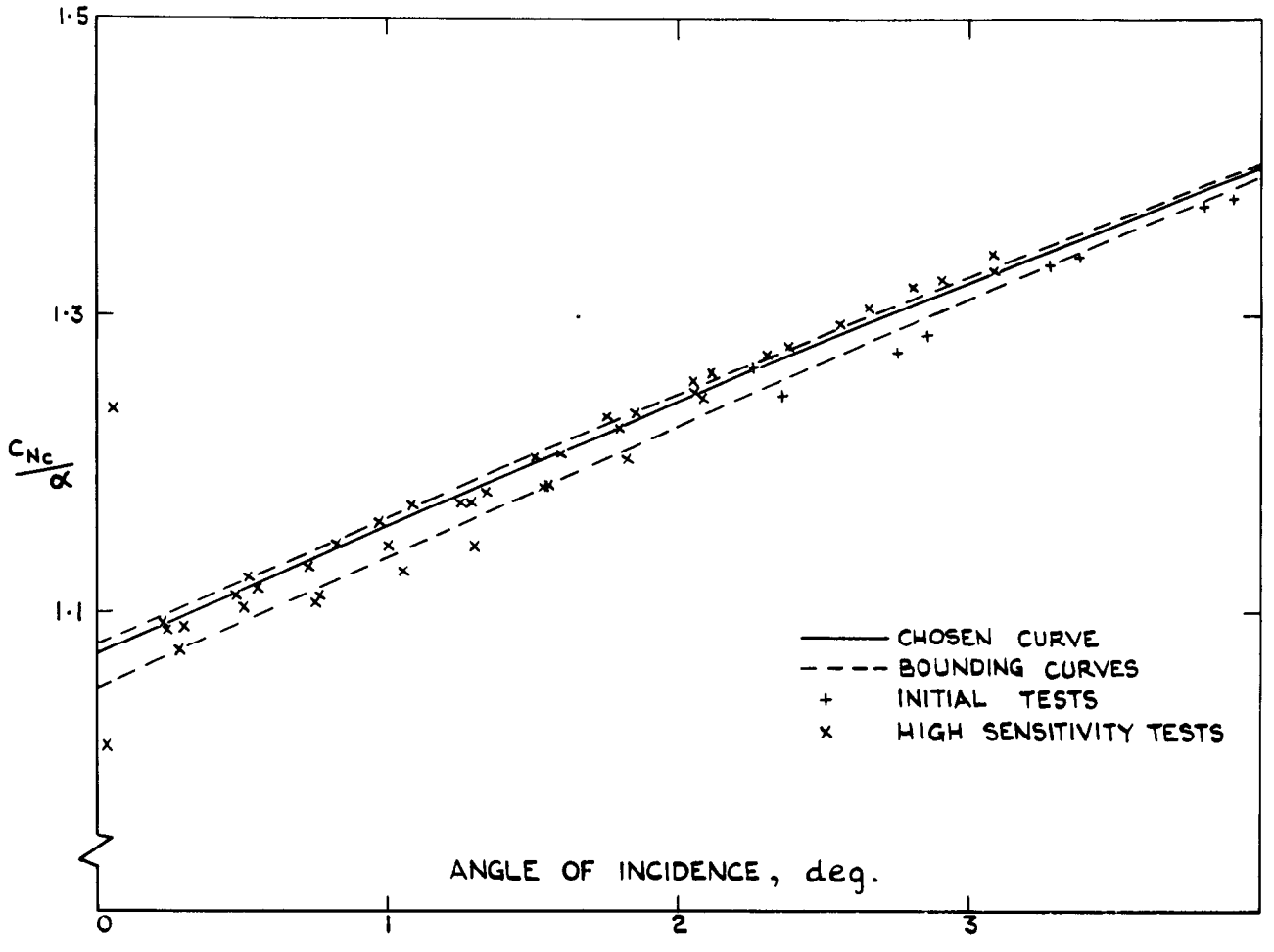

FIG.10 (a) VARIATION WITH INCIDENCE OF C_{Nc}/α FOR WING $\pi/6/0$

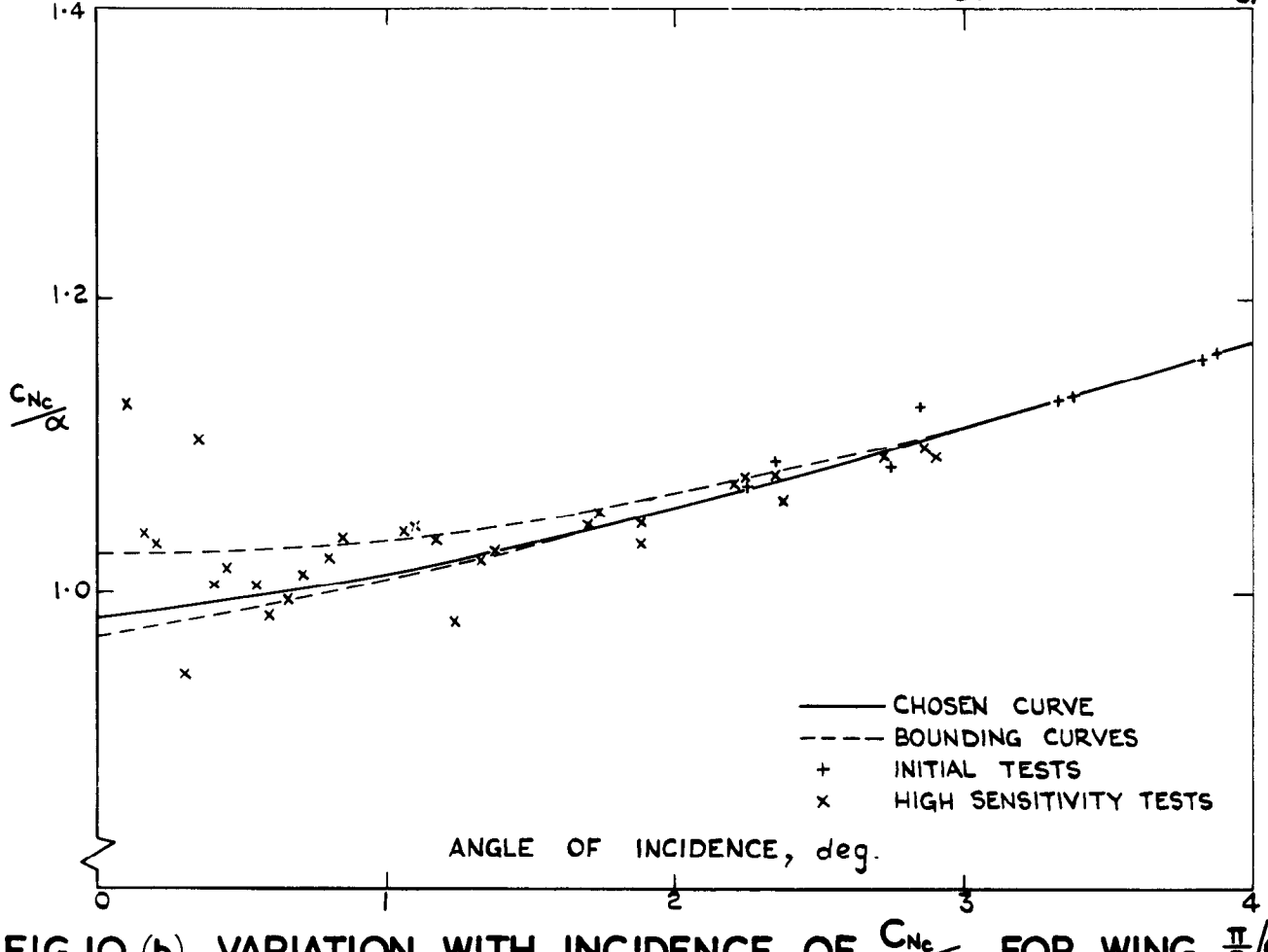

FIG.10 (b) VARIATION WITH INCIDENCE OF C_{Nc}/α FOR WING $\pi/3/0$

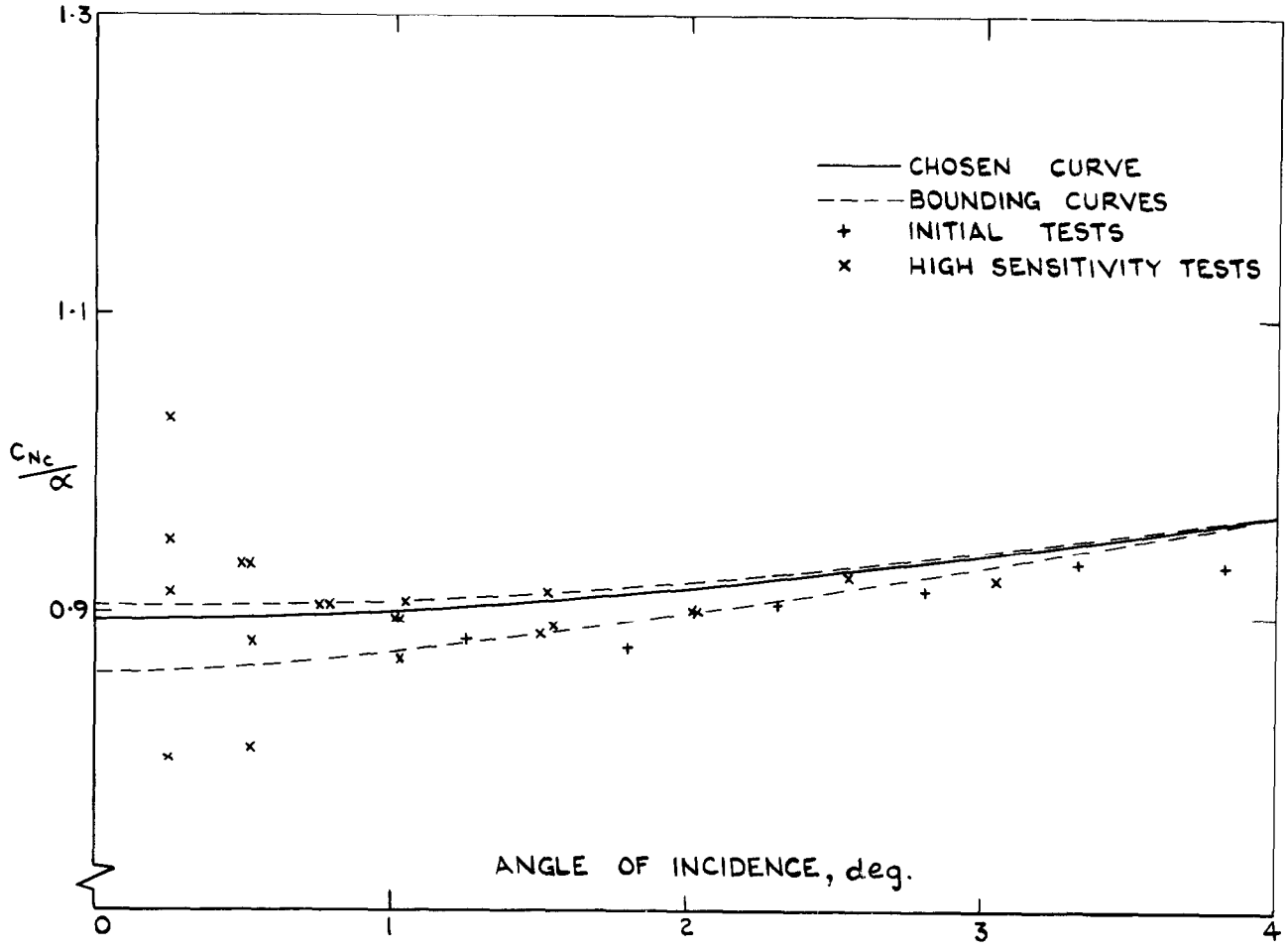

FIG. 10 (c) VARIATION WITH INCIDENCE OF C_{Nc}/α FOR WING $\frac{\pi}{2}/O$

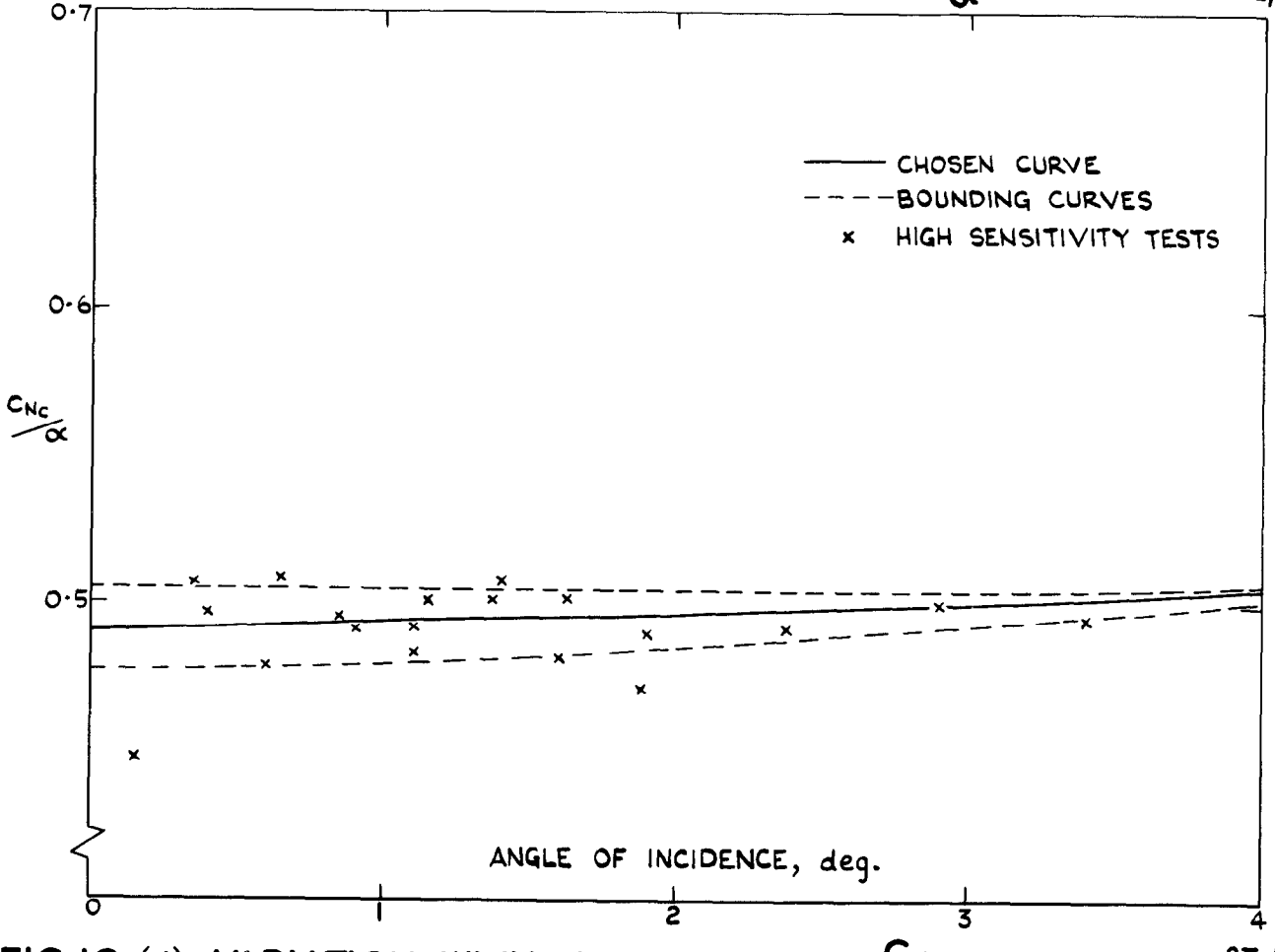

FIG. 10 (d) VARIATION WITH INCIDENCE OF C_{Nc}/α FOR WING $\frac{2\pi}{3}/O$

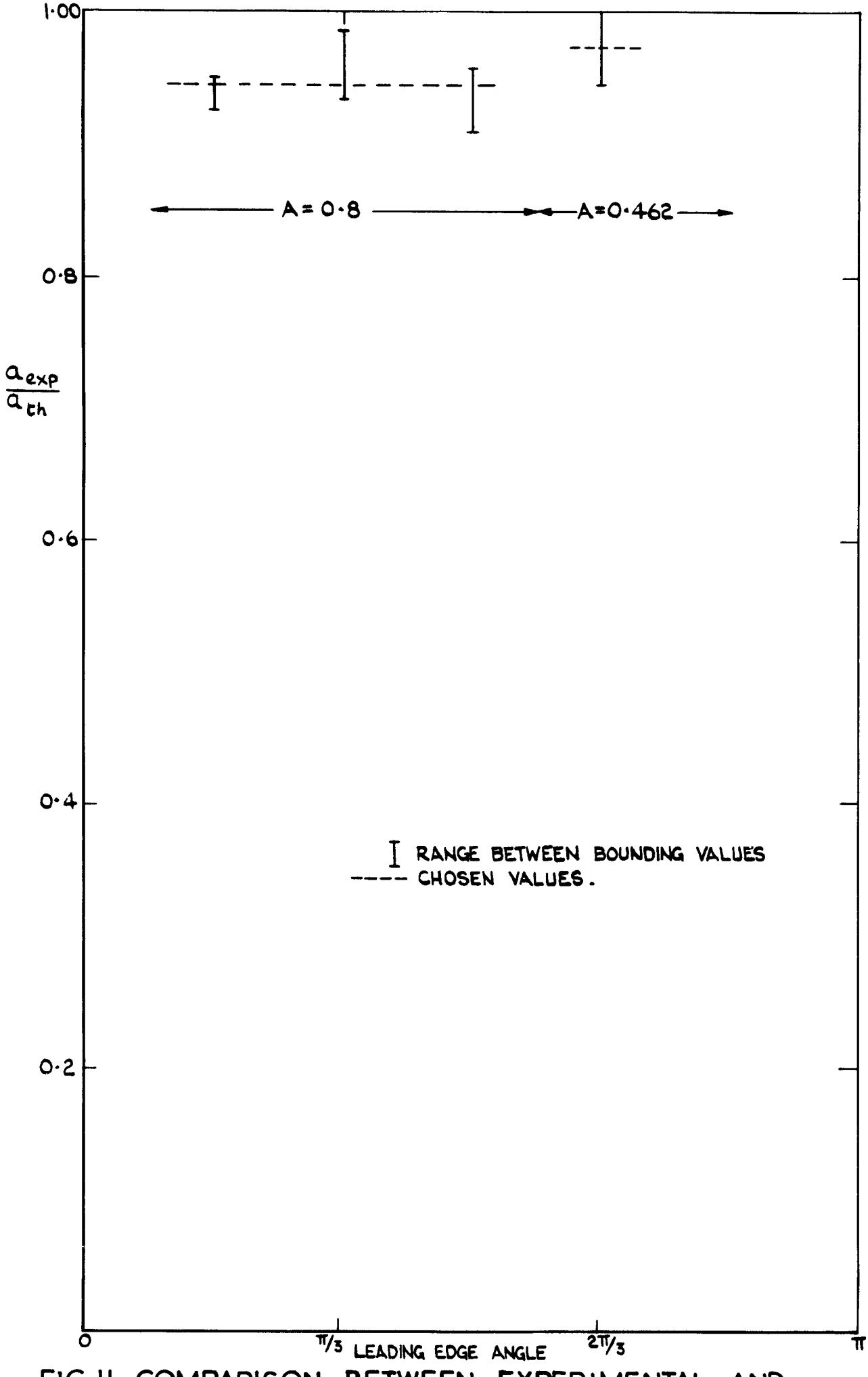

FIG. 11 COMPARISON BETWEEN EXPERIMENTAL AND THEORETICAL VALUES OF a

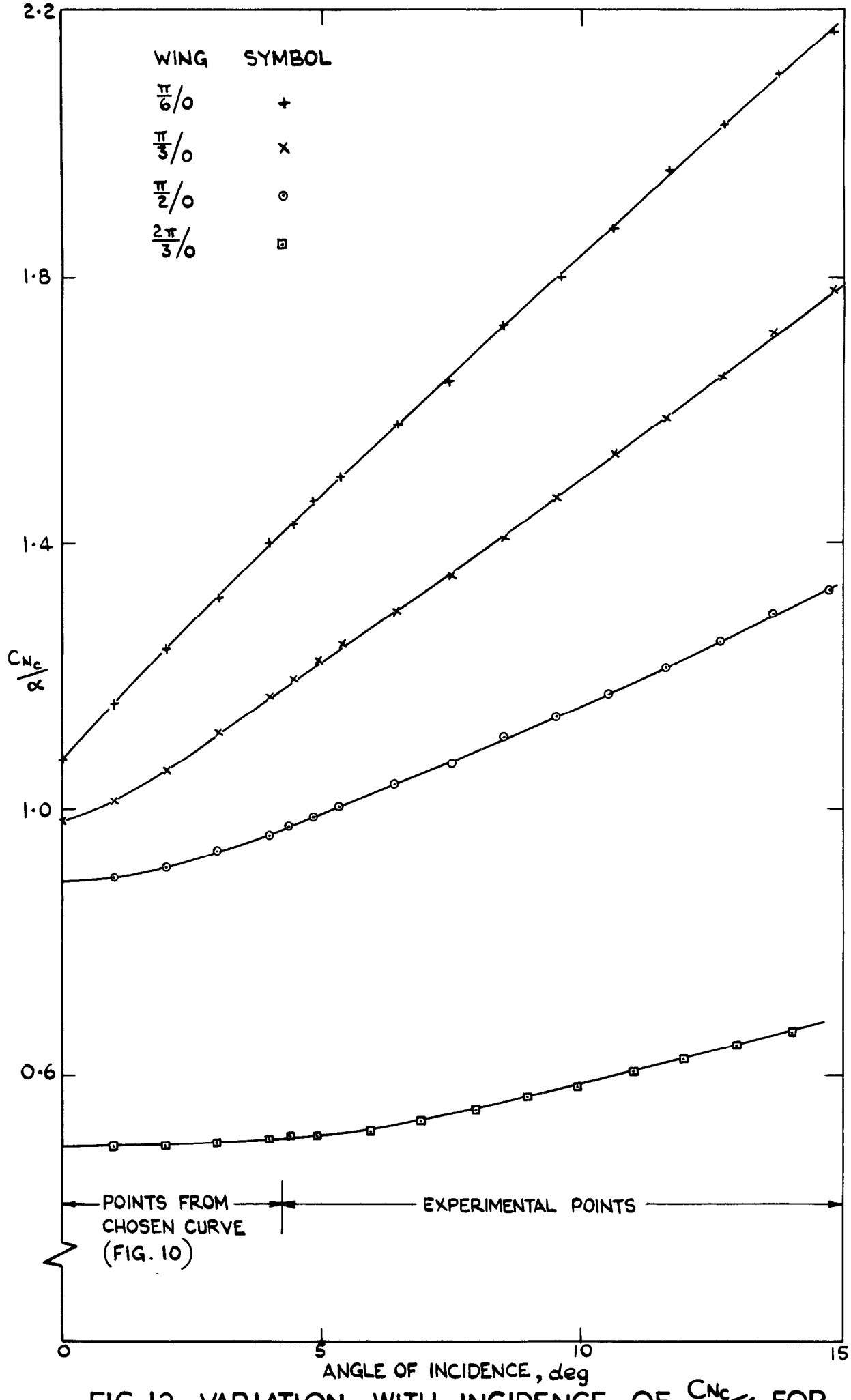

FIG. 12 VARIATION WITH INCIDENCE OF C_{N_c}/α FOR THE FOUR WINGS TESTED

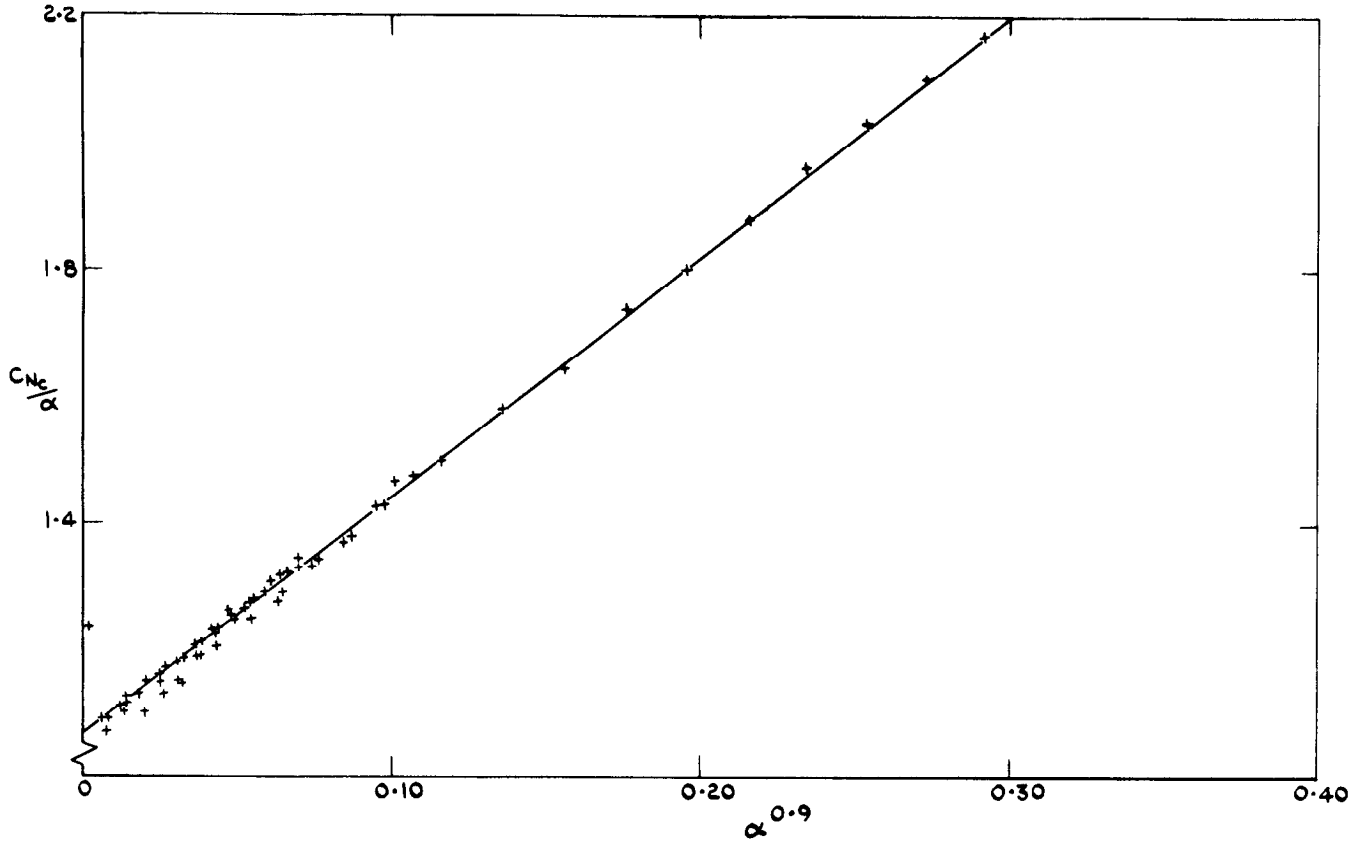

FIG. 13 (a) VARIATION OF C_{N_c}/α WITH $\alpha^{0·9}$ FOR WING $\frac{\pi}{6}/0$

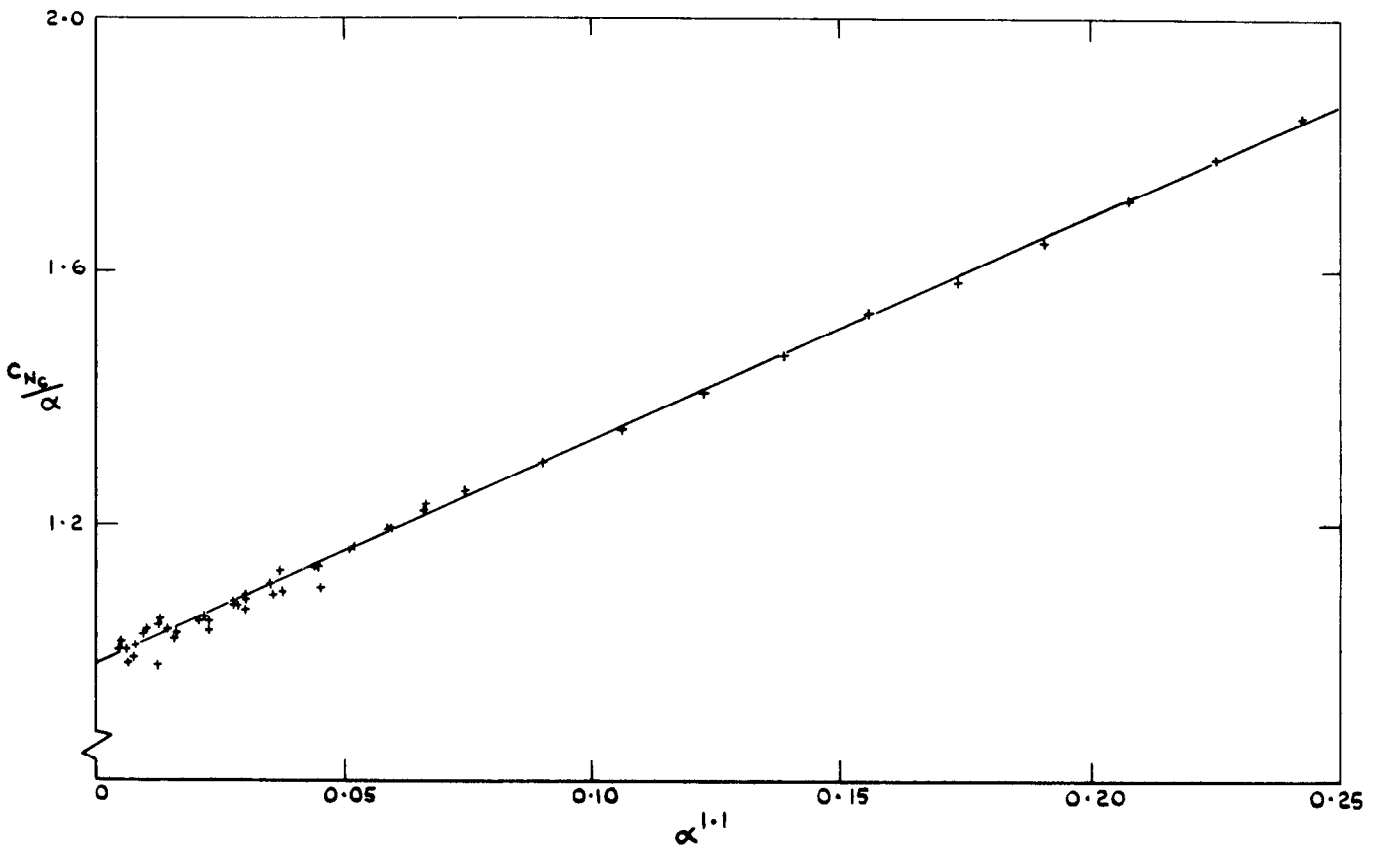

FIG. 13 (b) VARIATION OF C_{N}/α WITH $\alpha^{1·1}$ FOR WING $\frac{\pi}{3}/0$

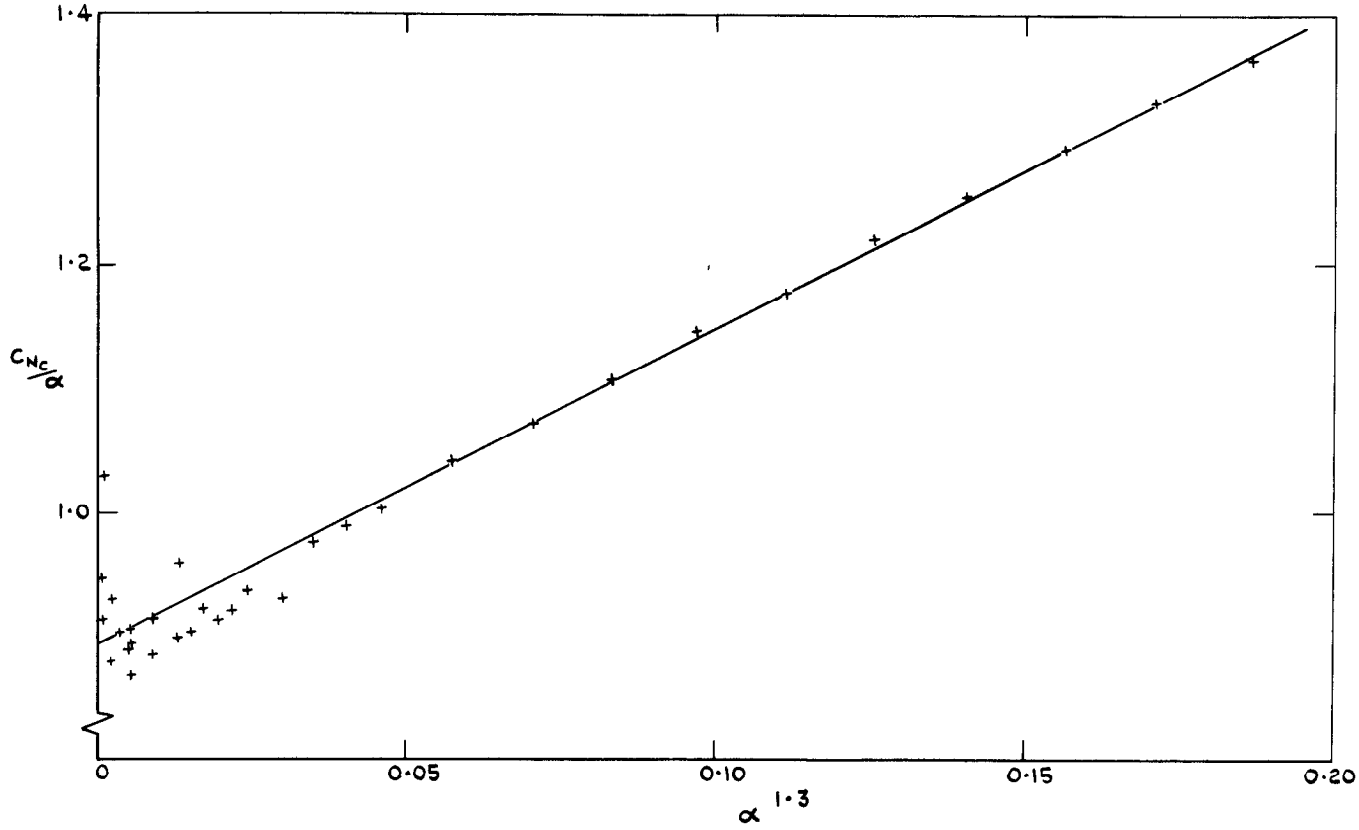

FIG. 13 (c) VARIATION OF C_{N_c}/α WITH $\alpha^{1·3}$ FOR WING $\frac{\pi}{2}/0$

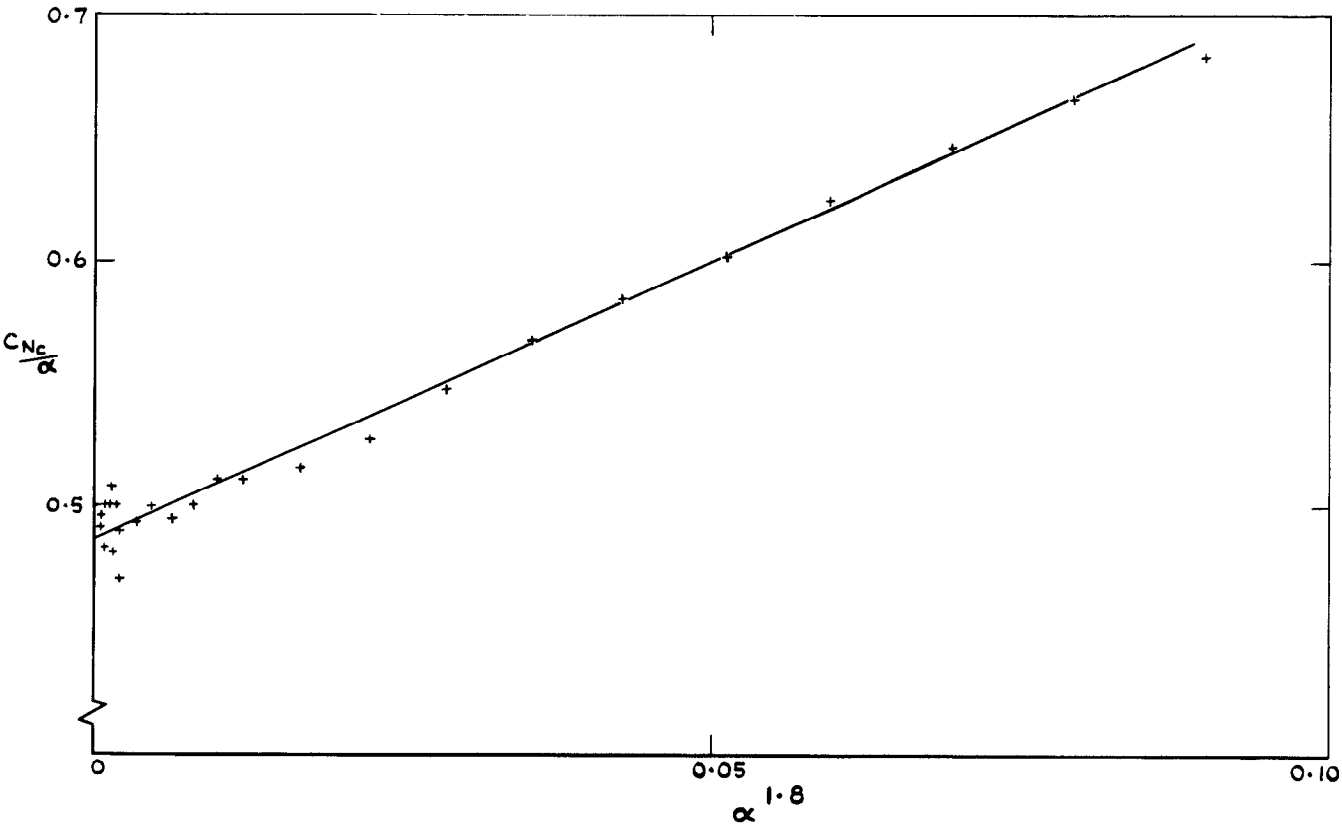

FIG. 13 (d) VARIATION OF C_{N_c}/α WITH $\alpha^{1·8}$ FOR WING $\frac{2\pi}{3}/0$

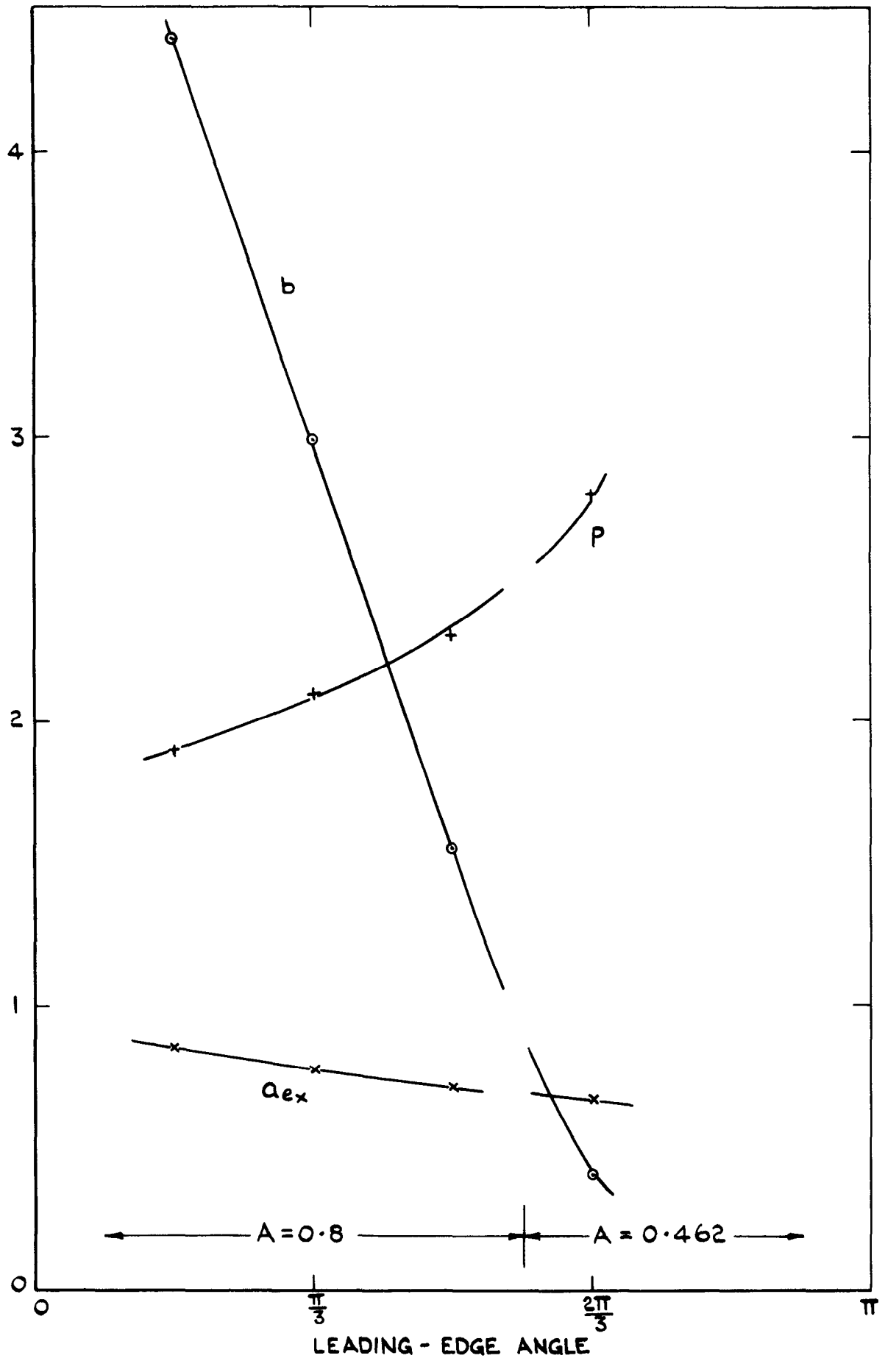

FIG. 14 VARIATION OF a_{ex}, b AND p WITH THE SIZE OF THE LEADING-EDGE ANGLE

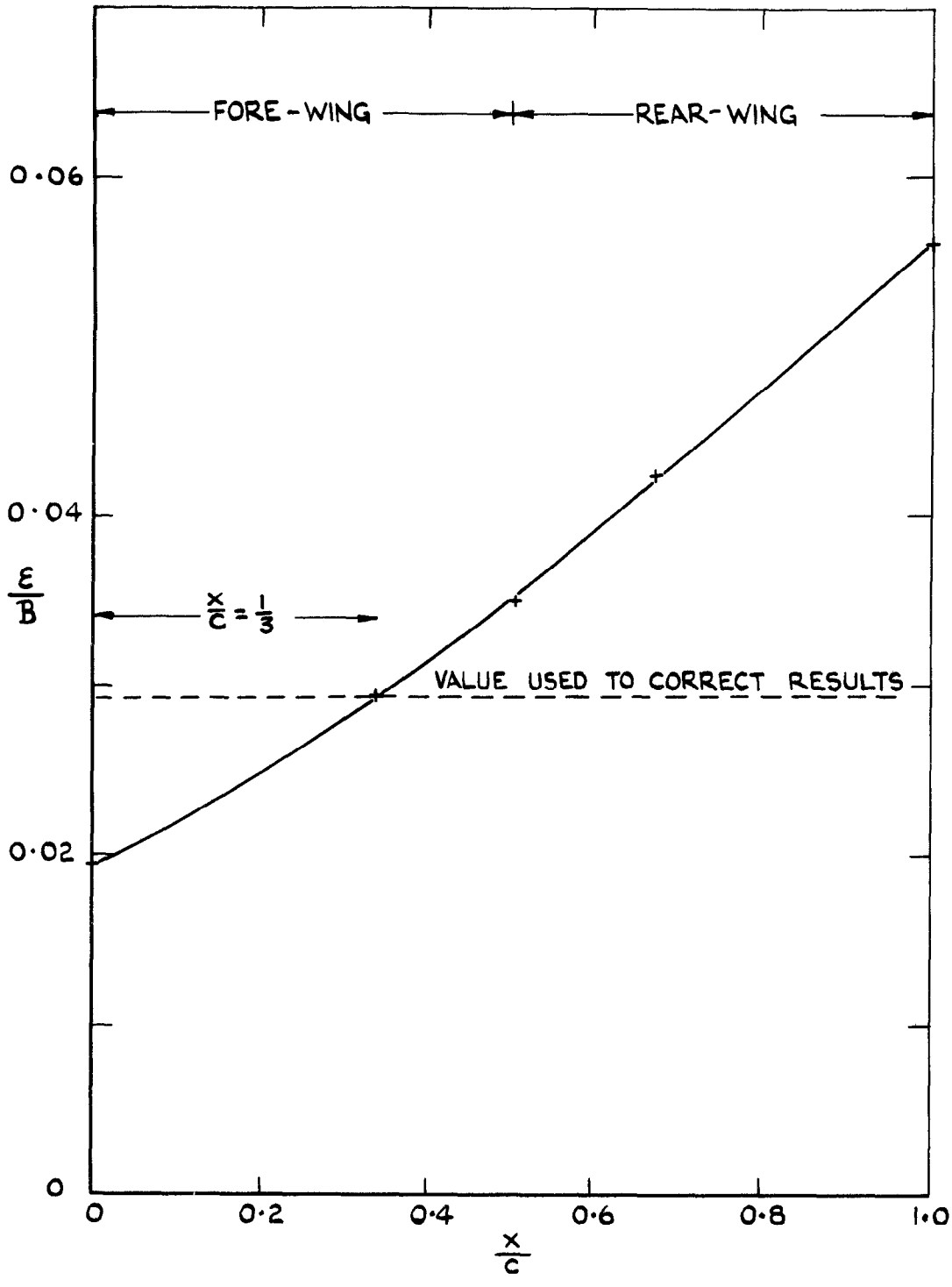

FIG.15 CHORDWISE DISTRIBUTION OF BLOCKAGE CORRECTION FOR CONICAL WINGS IN 4ft x 3ft WIND TUNNEL

Printed in England for Her Majesty's Stationery Office by the Royal Aircraft Establishment, Farnborough. Dd.125875 K.4

A.R.C. C.P. No.922
December 1965

Kirkpatrick, D. L. I.

533.693.3 :
533.6.013.13 :
533.692.2 :
532.517.43 :
533.6.011.32/34

INVESTIGATION OF THE NORMAL FORCE CHARACTERISTICS OF SLENDER DELTA WINGS WITH VARIOUS RHOMBIC CROSS-SECTIONS IN SUBSONIC CONICAL FLOW

This report describes an experimental technique which was developed to determine the aerodynamic normal forces associated with the conical flow fields round slender wings at incidence. With this experimental technique it is possible to obtain the accurate information necessary for the investigation of the theoretical similarity of the conical flow fields round slender wings with different cross-sectional shapes. The report presents the results of the tests on four low-aspect-ratio wings with rhombic cross-sections whose leading-edge angles were $\pi/6$, $\pi/3$, $\pi/2$ and $2\pi/3$. These results show that the development with incidence of the normal force is appreciably affected by the magnitude of the leading-edge angle. The normal force component associated with the leading-edge vortices,
(over)

A.R.C. C.P. No.922
December 1965

Kirkpatrick, D. L. I.

533.693.3 :
533.6.013.13 :
533.692.2 :
532.517.43 :
533.6.011.32/34

INVESTIGATION OF THE NORMAL FORCE CHARACTERISTICS OF SLENDER DELTA WINGS WITH VARIOUS RHOMBIC CROSS-SECTIONS IN SUBSONIC CONICAL FLOW

This report describes an experimental technique which was developed to determine the aerodynamic normal forces associated with the conical flow fields round slender wings at incidence. With this experimental technique it is possible to obtain the accurate information necessary for the investigation of the theoretical similarity of the conical flow fields round slender wings with different cross-sectional shapes. The report presents the results of the tests on four low-aspect-ratio wings with rhombic cross-sections whose leading-edge angles were $\pi/6$, $\pi/3$, $\pi/2$ and $2\pi/3$. These results show that the development with incidence of the normal force is appreciably affected by the magnitude of the leading-edge angle. The normal force component associated with the leading-edge vortices,
(Over)

A.R.C. C.P. No.922
December 1965

Kirkpatrick, D. L. I.

533.693.3 :
533.6.013.13 :
533.692.2 :
532.517.43 :
533.6.011.32/34

INVESTIGATION OF THE NORMAL FORCE CHARACTERISTICS OF SLENDER DELTA WINGS WITH VARIOUS RHOMBIC CROSS-SECTIONS IN SUBSONIC CONICAL FLOW

This report describes an experimental technique which was developed to determine the aerodynamic normal forces associated with the conical flow fields round slender wings at incidence. With this experimental technique it is possible to obtain the accurate information necessary for the investigation of the theoretical similarity of the conical flow fields round slender wings with different cross-sectional shapes. The report presents the results of the tests on four low-aspect-ratio wings with rhombic cross-sections whose leading-edge angles were $\pi/6$, $\pi/3$, $\pi/2$ and $2\pi/3$. These results show that the development with incidence of the normal force is appreciably affected by the magnitude of the leading-edge angle. The normal force component associated with the leading-edge vortices,
(Over)

which are characteristic of the flow round slender wings, develops much more slowly with incidence when the edge angle is large than when it is small. As the leading-edge angle is reduced, the slope of the normal force characteristic at zero incidence increases in the manner predicted by slender body theory, though the measured values are slightly smaller than those predicted.

which are characteristic of the flow round slender wings, develops much more slowly with incidence when the edge angle is large than when it is small. As the leading-edge angle is reduced, the slope of the normal force characteristic at zero incidence increases in the manner predicted by slender body theory, though the measured values are slightly smaller than those predicted.

which are characteristic of the flow round slender wings, develops much more slowly with incidence when the edge angle is large than when it is small. As the leading-edge angle is reduced, the slope of the normal force characteristic at zero incidence increases in the manner predicted by slender body theory, though the measured values are slightly smaller than those predicted.

Published by
HER MAJESTY'S STATIONERY OFFICE
To be purchased from
49 High Holborn, London W.C.1
423 Oxford Street, London W.1
13A Castle Street, Edinburgh 2
109 St. Mary Street, Cardiff
Brazennose Street, Manchester 2
50 Fairfax Street, Bristol 1
35 Smallbrook, Ringway, Birmingham 5
80 Chichester Street, Belfast 1
or through any bookseller

C.P. No. 922

S.O. CODE No. 23-9017-22